AD-A162 220 ANALYSIS OF PROGRESSIVE MATRIX CRACKING IN COMPOSITE LAMINATES(U) RENSSELAER POLYTECHNIC INST TROY NY DEPT OF CIVIL ENGINEERING G J DVORAK 31 MAR 85 1/1

UNCLASSIFIED AFOSR-TR-85-1064 AFOSR-82-0308 F/G 11/4 NL

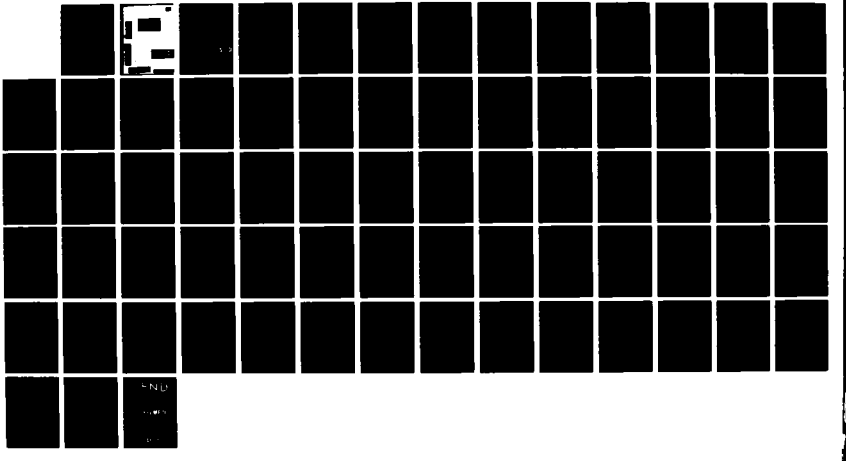

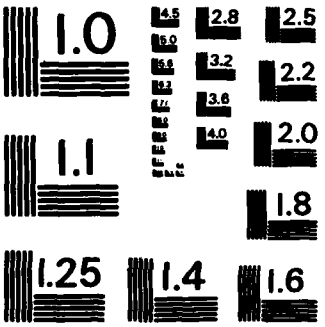

MICROCOPY RESOLUTION TEST CHART
NATIONAL BUREAU OF STANDARDS - 1963 - A

ANALYSIS OF PROGRESSIVE MATRIX CRACKING IN COMPOSITE LAMINATES

George J. Dvorak

(2)

FINAL REPORT

ANALYSIS OF PROGRESSIVE MATRIX CRACKING

IN

COMPOSITE LAMINATES

Approved for public release;
distribution unlimited.

George J. Dvorak

Department of Civil Engineering

Rensselaer Polytechnic Institute

Submitted to:

Air Force Office of Scientific Research

Bolling Air Force Base, Washington, DC

Contract AFOSR-82-0308

March 1985

TABLE OF CONTENTS

ABSTRACT

This report summarizes

A summary of recent results is presented on the subject of progressive ply cracking in fibrous laminates. ~~First,~~ evaluation of stiffness changes caused by systems of aligned slit cracks which are parallel to the fiber direction in a unidirectional composite lamina is discussed. Results obtained by the self-consistent method are presented. Next, a procedure for estimating instantaneous crack densities and stiffness changes in a lamina subjected to a prescribed strain history is outlined. These results are extended to analysis of laminated composite plates under in-plane stresses. Specific examples and comparisons of analytical and experimental results are presented for two graphite-epoxy systems.

Keywords: Composite materials; Cracking; Damage simulation.

1. STATEMENT OF WORK

In many fibrous composite systems the failure strain of the fiber far exceeds that of the matrix. Under load, the difference is usually accommodated by matrix cracking. This is frequently observed in monotonically or cyclically loaded laminated plates, where each layer may contain a system of aligned slit cracks which grow in the direction of the fibers and across the thickness of the ply. Such cracks are often called ply cracks or transverse cracks, although it is more appropriate to reserve the latter for cracks which are perpendicular to the fiber axis, and refer to cracks which grow parallel to the fiber direction as axial cracks.

In polymer matrix composites axial matrix cracking typically starts at low strain levels in the weakest off-axis ply. As loading continues, cracks appear in other off-axis plies; also, their density increases until it reaches a certain saturation level. For example, in statically loaded $(0/90)_s$ graphite-epoxy laminates the minimum crack spacing was observed to be equal to 3.5-4.0 ply thicknesses [1]. In metal matrix composites, matrix cracking appears to be caused only by cyclic loads which exceed the shakedown limit of the laminate [2]. Under such circumstances the matrix experiences cyclic plastic straining and, consequently, low-cycle fatigue failure. Both axial and transverse cracking is present, the former in off-axis plies, the latter in zero degree plies. The crack patterns and densities are generally similar to

those found in polymer matrix systems. However, saturation density increases with load amplitude, and it is not unusual to find cracks as close as one ply thickness.

In a typical part of a laminated composite structure, removed from concentrated loads and free edges, matrix cracking is the initial, low-stress damage mode under applied load. It is eventually followed by other types of damage, such as delamination between layers and fiber breaks; but these appear at relatively high loads which may exceed allowable design magnitudes. In contrast, matrix cracks grow at low loads, and they can significantly impair stiffness and strength of composite structures, especially those containing many off-axis plies. For example, fatigue tests on both polymer and metal matrix laminated plates indicate that stiffness and residual static strength reductions caused by cracking in plies may be as high as 10-50% after 2×10^6 cycles of loading [2,3]. It is therefore desirable to consider the effect of matrix cracking on composite properties in design.

Sufficiently general theoretical models of progressive cracking in composite laminates are apparently not to be found in the literature. Such results as are available for angle-ply laminates have been obtained from finite element calculations [1], while other studies have focused on $(0/90_n)_s$ laminates [4].

The purpose of this research is to develop a procedure for

prediction of crack densities in individual plies of a laminated composite structure as a function of applied load, and to evaluate the effect of cracks on stiffness of the structure.

The analysis has been performed in the following steps:

a) Evaluation of overall thermoelastic properties of a fibrous composite which contains a certain density of aligned slit cracks.

b) Evaluation of crack densities and stiffness changes in a single ply which is strained in a prescribed way.

c) Evaluation of crack densities and stiffness changes in a laminated composite plate which is subjected to prescribed loading. Specific examples were solved for laminated plates under in-plane loads. Comparisons of theoretical predictions was made with experimental data.

2. STIFFNESS CHANGES CAUSED BY A SYSTEM OF CRACKS IN A PLY

2.1 Preliminaries

We are concerned with evaluation of overall compliance, thermal expansion coefficients (or thermal strain and stress vectors), and strain and stress averages in the phases of a fibrous lamina which contains aligned slit cracks, and is subjected to uniform mechanical loads and thermal changes. The approach to the problem was outlined in reference [5], where we suggested that the effect of matrix crack systems on properties of fibrous composites can be analyzed, in principle, by the same techniques which are commonly used in evaluation of elastic constants of composite materials and fibrous laminates, e.g., by the self-consistent method.

The essential approximation in the evaluation of stiffness and compliance changes of laminates consists in the replacement of a cracked layer, Figure 1b, by an effective medium which contains many cracks, Figure 1a. The crack densities can be exactly matched to provide identical stiffnesses. However, the cracks in the layer are not entirely surrounded by the layer material, instead they interact with neighboring layers which have different elastic properties. This interaction is limited to the vicinity of the crack tip, thus it may be important in analysis of local crack growth at the interface, but it has

only a minor effect on lamina stiffness. We note that a similar approximation is commonly accepted in evaluation of elastic moduli of laminated composite structures reinforced by monolayers of large diameter fibers.

When the composite is reinforced by monolayers of fibers, such as boron or silicon carbide, the cracks and fibers may be of similar size. The appropriate model is shown in Figure 2. It is analogous to that of Figure 1, except that it contains three phases (fiber, matrix, and cracks), whereas the model of Figure 1 can be reduced to two phases (composite "matrix", and cracks). Accordingly, the models in Figures 1 and 2 are referred to as two-phase and three-phase models, respectively. From the practical standpoint, the effect of model choice on composite stiffness is small. The simpler two-phase model is thus sufficient for analysis of all fibrous systems.

In the three phase model we designated the fiber as phase 1, matrix as phase 2, and cracks as phase 3. In the two phase model phases 1 and 2 are joined in a homogeneous "matrix" and designated as phase 2; the voids or cracks remain phase 3.

The self-consistent analysis of the cracked composite, as outlied in [5-7], starts with a composite geometry in which the cracks are initially regarded as ellipsoidal cylindrical inclusions. A self-consistent estimate of overall stiffness of this medium is obtained. Next, the

inclusions are evacuated, i.e., replaced by voids. Finally, the aspect ratio of the voids is adjusted so that in the limit the voids change to cracks.

To evaluate crack density, the cracks in Figure 1 are first replaced by elliptic cylindrical voids, with a, b, denoting the major and minor semiaxes. If n is the number of voids per unit area in the x_1x_2-plane, then the volume fraction of voids is equal to $c_3 = \pi abn$, and $c_2 + c_3 = 1$. Next, let the voids be reduced to cracks, i.e., $\delta = b/a \to 0$. Then

$$c_3 = \pi a^2 n\delta = \frac{1}{4}\pi\beta\delta \qquad (1)$$

where $\beta = 4na^2$ is the crack density parameter. In fact, β is equal to the number of cracks of fixed length, e.g., 2a, in a square of side 2a. For example, if the cracks are located in a ply, Figure 1b, then β measures the distance between regularly spaced cracks in terms of ply thickness 2a. At $\beta = 1$, the distance between cracks is equal to 2a, as β *decreases* the distance *increases* and at $\beta = 0$ the cracks vanish. We recall that the observed minimum distances between cracks in a saturation state are equal to 3.5-4.0 ply thicknesses, i.e., 7a-8a [1]. Corresponding values of β are 0.28-0.25, but values as high as $\beta = 1$ were observed in the B-Al system [2]. Therefore $0 \leq \beta \leq 1$ is the appropriate range of β.

On the macroscale, the cracked unidirectional composite of Figure 1 can be regarded as an orthotropic homogeneous solid. The elastic properties of the "matrix" are identical with those of the fibrous composite and can be easily evaluated. When cracks are introduced, the macroscopic or overall elastic moduli of the solid change. To make the concept of overall moduli meaningful, it is necessary to consider overall uniform loading. Thus, we introduce uniform overall average stresses $\overline{\underset{\sim}{\sigma}}$ and strains $\overline{\underset{\sim}{\varepsilon}}$, with components arranged in (6x1) column vectors and related by constitutive equations*

$$\overline{\underset{\sim}{\sigma}} = L\,\overline{\underset{\sim}{\varepsilon}} \quad , \qquad \overline{\underset{\sim}{\varepsilon}} = M\,\overline{\underset{\sim}{\sigma}} \quad , \tag{2}$$

where L, and M are the overall stiffness, and compliance (6x6) matrices of the cracked composite, respectively. $M = L^{-1}$ when the inverse exists. Effective properties of uncracked fibrous material (phase 2) are denoted by L^0, M^0, or by L_2, M_2.

---

* As in [5-7], (6x6) matrices are denoted by capital Latin or Greek letters, e.g., L, M, Λ, A, B, P, Q, and (6x1) matrices by lower case bold face letters, e.g., $\underset{\sim}{\sigma}$, $\underset{\sim}{\varepsilon}$, m, $\underset{\sim}{\ell}$.

For a dilute concentration of aligned slit cracks, the matrices L and M can be evaluated by the self-consistent method. This was done in Reference [5]; the results are:

$$L = L_2 - \bar{\beta} L_2 \Lambda L \tag{3}$$

$$M = M_2 + \bar{\beta} \Lambda \quad , \tag{4}$$

where $L_2 = L^0$, $M_2 = M^0$, and

$$\bar{\beta} = \frac{1}{4} \pi \beta \quad . \tag{5}$$

The matrix Λ has only three nonzero components, which are expressed in terms of compliances M of the effective medium as:

$$\Lambda_{22} = \frac{M_{22}M_{33}-M_{23}^2}{M_{33}} (\alpha_1^{\frac{1}{2}} + \alpha_2^{\frac{1}{2}})$$

$$\Lambda_{44} = (M_{44}\, M_{55})^{\frac{1}{2}} \tag{6}$$

$$\Lambda_{66} = \frac{(M_{22}M_{33}-M_{23}^2)^{\frac{1}{2}}(M_{11}M_{33}-M_{13}^2)^{\frac{1}{2}}}{M_{33}} (\alpha_2^{\frac{1}{2}} + \alpha_2^{\frac{1}{2}})$$

where α_1 and α_2 are the roots of

$$(M_{22}M_{33}-M_{23}^2)\alpha^2 - \{M_{33}M_{66} + 2(M_{12}M_{33} - M_{13}M_{23})\}\alpha + M_{11}M_{33} - M_{13}^2 = 0 \tag{7}$$

These results imply that only three compliance coefficients M_{22}, M_{44}, and M_{66} are affected by the introduction of cracks, the remaining six terms in M are unchanged, i.e., they remain equal to those of the uncracked fiber composite. In particular

$$M_{11} = M^o_{11} \quad , \quad M_{12} = M^o_{12} \quad , \quad M_{13} = M^o_{13}$$

$$M_{23} = M^o_{23} \quad , \quad M_{33} = M^o_{33} \quad , \quad M_{55} = M^o_{55}$$

$$M_{22} = M^o_{22} + \overline{\beta}(M_{22}M_{33} - M^2_{23})(\alpha_1^{\frac{1}{2}} + \alpha_2^{\frac{1}{2}})/M_{33} \tag{8}$$

$$M_{44} = M^o_{44} + \overline{\beta}(M_{44}M_{55})^{\frac{1}{2}} \tag{9}$$

$$M_{66} = M^o_{66} + \overline{\beta}(M_{22}M_{33}-M^2_{23})^{\frac{1}{2}}(M_{11}M_{33}-M^2_{13})^{\frac{1}{2}}(\alpha_1^{\frac{1}{2}} + \alpha_2^{\frac{1}{2}})/M_{33} \tag{10}$$

and from (7):

$$\alpha_1\alpha_2 = (M_{11}M_{33}-M^2_{13})/(M_{22}M_{33}-M^2_{23})$$

$$\alpha_1 + \alpha_2 = [M_{33}M_{66} + 2(M_{12}M_{33}-M_{13}M_{23})]/[M_{22}M_{33}-M^2_{23}] \quad .$$

The unknown shear compliance M_{44} can be obtained directly from (9):

$$M_{44} = M^{o}_{44} + \frac{\overline{\beta}}{2}[\overline{\beta}\, M_{55} + (\overline{\beta}^2\, M^2_{55} + 4M^{o}_{44}\, M_{55})^{1/2}] \qquad (11)$$

The remaining unknowns M_{22} and M_{66} are found from (8) and (10).

These results can be utilized in (4) for a more direct evaluation of the three nonzero components of the matrix Λ in (6):

$$\Lambda_{ij} = (M_{ij} - M^{o}_{ij})/\overline{\beta} \quad . \quad (ij = 22, 44, 66) \qquad (12)$$

Of course, the same result follows from (6) and (7). In any case, the Λ_{ij} may now be substituted into (3), and the components of the overall stiffness L can be found in a closed form. The resulting expressions are given in reference [7, eqn. (A-6)].

It is seen that the results are remarkably simple, and similar to those that are routinely used for evaluation of elastic moduli of an uncracked composite medium. This similarity is particularly useful in applications of the results to laminated structures.

2.2 Response to Thermal Change

Let θ denote a uniform temperature change from a reference temperature θ_0, applied to the composite. The constitutive equation (2) must be replaced by

$$\underset{\sim}{\bar{\sigma}} = \underset{\sim}{L}\,\underset{\sim}{\bar{\varepsilon}} - \theta\underset{\sim}{\ell} \qquad \underset{\sim}{\bar{\varepsilon}} = \underset{\sim}{M}\,\underset{\sim}{\bar{\sigma}} + \theta\underset{\sim}{m} \quad , \tag{13}$$

where $\underset{\sim}{m}$ is the thermal expansion vector and $\underset{\sim}{\ell}$ the thermal stress vector. From (13) one obtains

$$\underset{\sim}{\ell} = \underset{\sim}{L}\,\underset{\sim}{m} \tag{14}$$

It is probably obvious that the presence of cracks does not affect free thermal expansion of the composite. Thus

$$\underset{\sim}{m} = \underset{\sim}{m}_0 \quad , \tag{15}$$

and from (3), (4) and (14):

$$\underset{\sim}{\ell} = (I - \beta L\Lambda)\underset{\sim}{\ell}_0 \tag{16}$$

Explicit forms of $\underset{\sim}{m}$ and $\underset{\sim}{\ell}$ are:

$$\underline{m} = \begin{bmatrix} \alpha_T \\ \alpha_T \\ \alpha_A \\ 0 \\ 0 \\ 0 \end{bmatrix} \quad ; \quad \underline{\ell} = \begin{bmatrix} (L_{11} + L_{12})\,\alpha_T + L_{13}\,\alpha_A \\ (L_{12} + L_{22})\,\alpha_T + L_{23}\,\alpha_A \\ (L_{13} + L_{23})\,\alpha_T + L_{33}\,\alpha_A \\ 0 \\ 0 \\ 0 \end{bmatrix} , \tag{17}$$

where α_T and α_A are linear thermal expansion coefficients of the uncracked composite in the transverse and axial directions, respectively. Since the coefficients of L_{ij} change with β, $\underline{\ell}$ is also a function of $\underline{m}$, while $\underline{m}$ remains constant.

Again, the derived expressions are valid only if the cracks are open. Closed cracks do not affect thermal response of the composite.

2.3 Local Strain and Stress Averages

Certain applications of the above results require information about local stress and strain fields in the phases. Estimates of local fields are also needed to distinguish between loading conditions which lead to either open or closed cracks and thus delineate limits of validity of the theory.

It is clear that when a fiber reinforced composite containing cavities is subjected to general uniform mecahnical loading, part of the applied strain (i.e., the average strain) is accommodated by cavity expansion. Whereas the strain of a typical cavity wall becomes unbounded in the limit of vanishing aspect ratio, the important quantity in the macroscopic study of composites is the wall strain multiplied by the area of the cross-section (or aspect ratio) which tends to a finite limit.

From the formulae given in [5,7], and in Section 2.2 above, it is not difficult to show that in the limit of slit cracks ($\delta \to 0$), the overall strain $\underset{\sim}{\bar{\varepsilon}}$ is given by

$$\underset{\sim}{\bar{\varepsilon}} = \underset{\sim}{\bar{\varepsilon}}_0 + \underset{\sim}{\bar{\varepsilon}}_c \quad , \tag{18}$$

where $\bar{\underline{\varepsilon}}_0$ is the average strain in the composite "matrix" :

$$\bar{\underline{\varepsilon}}_0 = (I - \bar{B} \wedge L)\bar{\underline{\varepsilon}} + \bar{B} \wedge L \underline{m} \theta \quad . \tag{19}$$

In addition, $\bar{\underline{\varepsilon}}_c$ is the <u>crack accommodation strain</u>

$$\bar{\underline{\varepsilon}}_c = \bar{B} \wedge L(\bar{\underline{\varepsilon}} - \underline{m}\theta) \quad ; \tag{20}$$

it represents that part of the applied (average) strain which is accommodated by cracks.

In practice equations (19) and (20) provide us with estimates of the local stress and strain fields within the composite.

Viewed from another standpoint, equations (19) and (20) immediately furnish the strain concentration factors. As far as the matrix is concerned,

$$\bar{\underline{\varepsilon}}_0 = A \bar{\underline{\varepsilon}} - \theta \underline{a} \tag{21}$$

where

$$A = I - \bar{B} \wedge L \tag{22}$$

$$\underline{a} = (A_0 - I) \underline{m} = - \bar{B} \wedge L \underline{m}$$

It is perhaps important to emphasize the different physical interpretations of $\bar{\underset{\sim}{\varepsilon}}_o$ and $\bar{\underset{\sim}{\varepsilon}}_c$. Whereas $\bar{\underset{\sim}{\varepsilon}}_o$ is the average strain in the matrix, $\bar{\underset{\sim}{\varepsilon}}_c$ represents that part of the overall strain which is accommodated by all the cracks. Therefore, one can write (20) as

$$\bar{\underset{\sim}{\varepsilon}}_c = \underset{\sim}{A}_c \bar{\underset{\sim}{\varepsilon}} - \theta \underset{\sim}{a}_c \quad , \tag{23}$$

where

$$\begin{aligned} A_c &= \bar{\beta} \Lambda L \\ \underset{\sim}{a}_c &= \bar{\beta} \Lambda L \underset{\sim}{m} \quad . \end{aligned} \tag{24}$$

For example, it is immediately obvious that the average thermal strains in a fully constrained cracked composite ($\bar{\underset{\sim}{\varepsilon}} = \underset{\sim}{0}$) are

$$\bar{\underset{\sim}{\varepsilon}}_o = - \bar{\underset{\sim}{\varepsilon}}_c = \bar{\beta} \Lambda L \underset{\sim}{m} \theta \quad .$$

The matrix expands at the expense of crack closing.

For computational purposes it is advantageous to rewrite (22_1) with the help of (3) in the form

$$A = M_o L \quad . \tag{25}$$

It is often convenient to have explicit forms of the above results.

The nonzero components of A in (22) are:

$$
\begin{aligned}
A_{11} &= A_{33} = A_{55} = 1 \\
A_{21} &= (M^{o}_{22} - M_{22})\, L_{12} \\
A_{22} &= (M^{o}_{22} - M_{22})\, L_{22} + 1 \\
A_{23} &= (M^{o}_{22} - M_{22})\, L_{23} \\
A_{44} &= M^{o}_{44}/M_{44} \\
A_{66} &= M^{o}_{66}/M_{66} \quad .
\end{aligned}
\tag{26}
$$

Again, M_{ij} are compliances of the uncracked composite.

The components of thermal strain concentration factor $\underline{a}$ in (22) are all zero, except for

$$
a_{22} = -\bar{B}\, \Lambda_{22}\, [(L_{12} + L_{22})\alpha_T + L_{23}\, \alpha_A] \tag{27}
$$

The average strain $\bar{\underline{\varepsilon}}_c$ (20), (23) in the cracks has the following nonvanishing components:

$$
\bar{\varepsilon}^{c}_{22} = \bar{B}\, \Lambda_{22} [L_{12}(\bar{\varepsilon}_{11} - \alpha_T \theta) + L_{22}(\bar{\varepsilon}_{22} - \alpha_T \theta) + L_{23}(\bar{\varepsilon}_{33} - \alpha_A \theta)] \tag{28}
$$

$$
\bar{\varepsilon}^{c}_{23} = (1 - M^{o}_{44}/M_{44})\bar{\varepsilon}_{23} \qquad \varepsilon^{c}_{12} = (1 - M^{o}_{66}/M_{66})\bar{\varepsilon}_{12} \quad ,
$$

We note that the distinction between open and closed cracks is determined by the inequality

$$
\varepsilon^{c}_{22} > 0 \quad , \tag{29}
$$

which can be evaluated with the help of (28).

The results presented here are valid only if this inequality is satisfied. If the sign is reversed, or if the two sides are equal, then cracks are closed and do not affect the mechanical and thermal response of the composite. An exception arises when the closed crack faces slide in shear. Treatment of this case is beyond the scope of the present paper.

Finally, we note that evaluation of stress averages in the phases is trivial. Since open cracks do not support any stress.

$$\bar{\underline{q}}_0 \equiv \bar{\underline{q}} \quad , \quad \bar{\underline{q}}_c \equiv \underline{0} \quad . \tag{30}$$

2.4 Stiffness at Large β

When a fibrous lamina is embedded in a laminated structure, it may crack rather extensively. Under such circumstances, certain components of L_{ij} in (3) become independent of β, or equal to zero. It is worth evaluating these limiting stiffnesses since they correspond to the worst possible damage to a particular ply of a laminate. A good approximation to the actual residual stiffness can be obtained as

$$L^*_{ij} = \lim_{\beta \to \infty} L_{ij} \quad . \tag{31}$$

Now as $\beta \to \infty$ it is easy to see that

$$M_{22},\ M_{44},\ M_{66} \to \infty$$

whereas the remaining components of the compliance matrix remain finite (and equal to the uncracked value). It then follows from simple matrix inversion that

$$\begin{aligned}
L^*_{11} &= M^o_{33}/\gamma = L^o_{11} - (L^o_{12})^2/L^o_{22} \\
L^*_{12} &= 0 \qquad L^*_{22} = 0 \qquad L^*_{23} = 0 \\
L^*_{13} &= -M^o_{13}/\gamma = L^o_{13} - L^o_{12}L^o_{23}/L^o_{22} \\
L^*_{33} &= M^o_{11}/\gamma = L^o_{33} - (L^o_{23})^2/L^o_{22}
\end{aligned} \tag{32}$$

where $\gamma = M^o_{11} M^o_{33} - (M^o_{13})^2$. Also,

$$L^*_{55} = L^o_{55} \quad , \quad L^*_{44} = L^*_{66} = 0 \quad . \tag{33}$$

For a moderately cracked ply, say $\beta = 1$, a reasonable approximation to the stiffnesses L_{ij} ($ij = 1,2,3$) is still given by (32), while L_{55} is of course equal to L^o_{55}. However, L_{44} and L_{66} must be calculated either directly from (3), or indirectly from (8), (10), and (11).

2.5 Selected Results

To illustrate the evaluation of compliances of a cracked composite, and of the "matrix" strain averages, we consider a T300 Gr-Ep system. Table I lists the constituent properties of fiber and matrix, and of the uncracked composite. The composite compliances were obtained from self-consistent estimates of moduli.

Figure 3 shows changes in the three compliances M_{22}, M_{44}, and M_{66}, calculated from Equations (8) - (11) for given values of crack density β. Of course, all these components increase with increasing β, but their change is quite gradual, especially at low β. This contrasts but is not in conflict with the relatively rapid reduction in stiffnesses which we found in [5].

We note that the composite without cracks is transversely isotropic, and has five independent compliances, M_{ij}. When cracks are introduced the coefficient M_{22}, M_{44}, and M_{66} change, the material is no longer transversely isotropic, and the number of independent elastic compliances increases to eight.

The changes caused by β in components of strain concentration factor A in (22) are shown in Figure 4. As required by (26), five of the eight components of A change with β. Note that the fiber volume fraction appears to have a small effect on A_{ij}. However, crack density β can have a significant effect on the strain concentration factor components, especially at relatively low values of β.

3. PROGRESSIVE MATRIX CRACKING IN A PLY

3.1 Preliminaries

Consider a unidirectionally reinforced composite ply of thickness 2a, which is embedded in a laminated plate, shell, or a similar composite composite structure. The structure is subjected to a certain incremental loading program which, at each loading step, causes a known instantaneous overall strain state $\bar{\underset{\sim}{\varepsilon}}$ in the ply under consideration. The strains $\bar{\varepsilon}_{ij}$ are assumed to be uniform within the ply. An element of the composite structure which contains the ply is shown in Fig. 5. A typical ply is bonded to laminated layers of thickness b' and b" such that at least one of the adjacent layers is much thicker than the ply, if b' > b" > 0, then b' > 2a.

At a certain magnitude of applied strain $\bar{\underset{\sim}{\varepsilon}}$, which is usually much smaller than the failure strain of the fiber, a system of matrix cracks starts to develop in the ply. The geometry of matrix cracks is influenced by the strength anisotropy of the fibrous ply, and by the state of stress. Clearly, cracks may propagate most easily on planes which are parallel to the fiber direction. An unbroken ply segment in a typical part of a laminated plate or shell, which is removed from free edges and other stress concentrations, usually supports a state of plane stress. In the coordinates of Figure 5, this suggests that components σ_{22}, σ_{23}, and σ_{33} are large in comparison to σ_{11}. Matrix cracks parallel to fibers are not affected by σ_{33}, although this stress component may cause cracking on planes perpendicular to fibers. The remaining stresses

favor cracking on x_1x_3-planes. The shear components σ_{12} and σ_{13} may be present as well, for example in bent plates where their magnitude varies through plate thickness. Again, σ_{13} does not influence axial cracks parallel to the fiber; σ_{12} contributes to crack growth on x_1x_3-planes, even though an exceptionally large σ_{12} might cause cracking on planes inclined to x_1 axis.

These considerations suggest that the matrix crack system consists of aligned slit cracks of width 2a, which are infinitely long in the fiber direction x_3.

The average spacing of cracks in the system can be conveniently described in terms of the crack density parameter β, the average distance between cracks is $2a/\beta$, Figure 5.

Of course, the actual spacing of cracks at a given value of β need not be regular. Available experimental observations suggest that individual cracks are initiated at randomly distributed locations in the ply, and then propagate, sometimes in an unstable manner, across the ply width [2,4]. The number of these cracks grows progressively with increasing $\bar{\varepsilon}$, up to a certain saturation, density, typically $\beta \leq 1$. Under sustained or cyclic loading the crack density may increase with time, even at a constant stress amplitude.

Regardless of the underlying fracture mechanism, the random crack pattern corresponding to a given average density β can be illustrated by the sequence of Figure 6. A ply segment of length ℓ = 12.5 mm and

thickness 2a = 0.125 mm is shown. The width of the segment is assumed to be much larger than 2a. In agreement with experimental observations, we assume that the actual distance between any two adjacent cracks cannot be smaller than the ply thickness 2a [2-4]. Thus, the 12.5 mm long segment can contain at most 100 cracks at $\beta = 1$. To illustrate the progressive cracking process, the possible crack locations in the ply segment at $\beta = 1$ were fixed at regular intervals, 2a apart. Then, a sequence of 100 random numbers was generated and each number was assigned to one of the prospective locations. Four values of β were selected, and at each β the required number of cracks was drawn in the locations with the lowest random numbers. For example, at $\beta = 0.1$ there are ten cracks in the segment. These are retained in their positions and supplemented by 20 additional cracks at $\beta = 0.3$, etc.

The sequence shown in Figure 6 was constructed, under the assumption that formation of a new crack is not influenced by the presence of an existing crack. Due to stress relaxation next to an existing crack, this may not be the case in an actual ply. At low values of β cracks may form preferentially at locations removed from existing cracks, and the crack distribution in the early stages of the process may become somewhat more uniform than that suggested by Figure 6.

3.2 Crack Interaction

Before the onset of cracking, the local strain and stress fields in a typical segment of a thin ply, removed from concentrated forces and free edges, are usually uniform. If the current applied strain $\bar{\underset{\sim}{\varepsilon}}$, and uniform thermal change θ are known, then the corresponding ply stress $\bar{\underset{\sim}{\sigma}}$ follows from constitutive equations (13).

Once a particular ply begins to crack, the uniform strain and stress fields are perturbed. There are stress singularities at crack tips, and the stress components $\bar{\sigma}_{22}$, $\bar{\sigma}_{13}$, and $\bar{\sigma}_{23}$ vanish on each crack face. Nevertheless, the crack affected regions are localized in the neighborhood of each crack. Thus in the early stages of cracking, each crack can be regarded as essentially isolated. In other words, the elastic field in the neighborhood of a particular crack can be determined by considering that crack alone in the ply.

As the crack density increases, so does the totality of perturbed regions. Ultimately, the cracks will interact with each other, and the crack-affected regions will eventually occupy the entire volume of the ply.

It is important to estimate the distance between cracks at which crack interaction becomes significant. One way of doing this is to consider a ply with an average crack density β, and investigate the differences between compliances $\underset{\sim}{M}$ obtained for interacting and noninteracting cracks. It is easy to anticipate that crack interaction

will cause major deviation from linearity in the M_{22} component which changes most rapidly with crack density β; c.f., Figure 3.

Specifically, with reference to Equation (4), the compliance for interacting cracks is:

$$M_{22} = M_{22}^{o} + \frac{1}{4} \pi \beta \Lambda_{22} \tag{34}$$

For noninteracting cracks, M_{22} is given by the linear formula

$$M'_{22} = M_{22}^{o} + \frac{1}{4} \pi \beta \Lambda_{22}^{o} \tag{35}$$

where M_{22}^{o}, Λ_{22}^{o} are values of M_{22}, Λ_{22} at $\beta = 0$.

The difference between the above compliances can be expressed in terms of $(M_{22} - M'_{22})/M'_{22}$. The following presents this ratio for the graphite-epoxy ply considered in Table I; the magnitudes are not dependent on fiber volume fraction c_f for $0.2 \leq c_f \leq 0.6$.

β	0.10	0.15	0.20	0.25	0.30	0.40	0.50
$(M_{22}-M'_{22})/M'_{22}$	0.017	0.038	0.068	0.105	0.151	0.271	0.432

These results, which apply to cracks already in existence, suggests that significant crack interaction starts at $\beta = 0.25$, when the compliance deviation from linearity becomes larger than 10%.

The concept of crack interaction needs to be understood from the stand-point of new crack formation in a volume of a ply which already has an average crack density β. If a crack which is about to form is found in a ligament between two existing cracks, it can be regarded as noninteracting only if the existing cracks are at least 8 or more ply thicknesses apart, i.e. when $\beta \leq 0.125$ before the crack forms.

Of course, crack initiation at random locations leads to considerable variations in local spacing. As suggested by Figure 6, individual cracks may be much closer than ply thicknesses at $\beta = 0.125$. Therefore, one can conclude that crack interaction starts very early in the cracking process. Indeed, assume that crack interaction is present for all values of $\beta > 0$.

3.3 Progressive Cracking of a Ply

In agreement with the conclusions reached in Section 3.2, we regard the progressive cracking process as a sequence of events in which individual cracks are initiated at random locations in the ply, and propagate, possibly in an unstable manner across the entire loaded width of the ply. Formation of a single crack represents an elementary step in the process. To account for interaction between cracks, we assume that the stress which causes the crack to form at a given average crack density β in the ply is equal to the volume average (13). Explicit form of relevant components is:

$$\bar{\sigma}_{12} = 2L_{66}\,\bar{\varepsilon}_{12} = 2L^{0}_{66}\,\bar{\varepsilon}_{12}(1 + \bar{\beta}\,L^{0}_{66}\,\Lambda_{66})^{-1}$$

$$\bar{\sigma}_{22} = L_{12}(\bar{\varepsilon}_{11} - \alpha_T\theta) + L_{22}(\bar{\varepsilon}_{22} - \alpha_T\theta) + L_{23}(\bar{\varepsilon}_{33} - \alpha_A\theta) \qquad (36)$$

$$= [L^{0}_{12}(\bar{\varepsilon}_{11} - \alpha_T\theta) + L^{0}_{22}\,(\bar{\varepsilon}_{22} - \alpha_T\theta) + L^{0}_{23}(\bar{\varepsilon}_{33} - \alpha_A\theta)]\,(1+\bar{\beta}\,L^{0}_{22}\Lambda_{22})^{-1}$$

$$\bar{\sigma}_{23} = 2L_{44}\bar{\varepsilon}_{23} = 2L^{0}_{44}\bar{\varepsilon}_{23}(1 + \bar{\beta}\,L^{0}_{44}\Lambda_{22})^{-1}$$

Fracture criteria for crack formation during progressive cracking are apparently not to be found in the literature. However, it is reasonable to expect that the process will be essentially repetitive, governed by a criterion similar to that for first ply failure.

In general, each slit crack in the ply can open in three modes, each of which corresponds to one of the three stresses (36). To fix ideas, consider that the slit crack extends in the direction parallel to

the fiber axis x_3, Figure 5. Then $\bar{\sigma}_{12}$ in (36) causes Mode III failure, $\bar{\sigma}_{23}$ Mode II, and $\bar{\sigma}_{22}$ Mode I. Mode III can be excluded in most applications, on the grounds that the fracture surface in a fibrous ply contains numerous longitudinal asperities created by the crack as it finds its way between densely packed fibers. These asperities are interlocked and thus prevent relative shear displacement of fracture surfaces in the x_1 direction. Of course, Mode III and $\bar{\sigma}_{12}$ are implicitly absent in plane stress.

Modes I and II are usually interrelated, but to a different extent in different composite systems. A ply failure criterion which reflects this fact way presented by Hahn et al. [8] for the case of $\bar{\sigma}_{22} > 0$, $\bar{\sigma}_{23} \neq 0$ in the form:

$$(1-g)(\bar{\sigma}_{22}/\bar{\sigma}_I) + g(\bar{\sigma}_{22}/\bar{\sigma}_I)^2 + (\bar{\sigma}_{23}/\bar{\sigma}_{II})^2 = 1 \qquad (37)$$

where g is an empirical interaction parameter, $0 < g \leq 1$. For $g = 1$ there is no interaction and (37) is reduced to the familiar quadratic form. The $\bar{\sigma}_I$ and $\bar{\sigma}_{II}$ are critical stresses at which the ply actually fails. These stresses increase with decreasing ply thickness. Also, as β grows, one expects that formation of new cracks may become gradually more difficult. This can be reflected by demanding that $\bar{\sigma}_I$, $\bar{\sigma}_{II}$ be nondecreasing functions of β. Thus we write:

$$\bar{\sigma}_I = \bar{\sigma}_I(a,\beta), \qquad \bar{\sigma}_{II} = \bar{\sigma}_{II}(a,\beta) \qquad (38)$$

While (37) is valid for $\bar{\sigma}_{22} > 0$, the composite ply may also crack if $\bar{\sigma}_{22} \leq 0$ and $\bar{\sigma}_{23} \neq 0$. Under such circumstances (37) should be replaced by

$$(\bar{\sigma}_{23}/\bar{\sigma}_{II})^2 = 1, \tag{38}$$

with $\bar{\sigma}_{II} = \bar{\sigma}_{II}(a, \beta, \bar{\sigma}_{22})$.

The critical stress magnitudes in (37) and (38) need to be established experimentally. So far, only first ply failure magnitudes of strengths (38) have appeared in the literature, c.f., [3,4]. Information about $\bar{\sigma}_{II}$, especially under compression (39), is generally not available.

If (12), (14) or an equivalent criterion is accepted for progressive cracking, then the average crack density β can be evaluated during incremental deformation of the ply. Suppose that the composite ply is subjected to current uniform strain $\bar{\underset{\sim}{\varepsilon}}$, and that the corresponding crack density is $\beta_0 > 0$. A strain increment $d\bar{\underset{\sim}{\varepsilon}}$, and a uniform thermal change $d\theta$ are applied, and a new magnitude of β is sought.

Let

$$\bar{\underset{\sim}{\varepsilon}} = \bar{\underset{\sim}{\varepsilon}} + d\bar{\underset{\sim}{\varepsilon}}, \qquad \theta' = \theta + d\theta \tag{40}$$

be the new values of strain and temperature. The corresponding average stress in the ply is, in analogy with (13):

$$\underset{\sim}{\bar{\sigma}}' = L' \underset{\sim}{\bar{\varepsilon}}' + \theta' \underset{\sim}{\ell}', \tag{41}$$

where $L' \equiv L'(\beta)$, $\underset{\sim}{\ell}' \equiv (\beta)$ are overall instantaneous material properties of the cracked ply at the as yet unknown value of

$$\beta = \beta_0 + d\beta;\ d\beta > 0. \tag{42}$$

To determine if $d\underset{\sim}{\bar{\varepsilon}}$ and $d\theta$ in (40) will actually cause additional cracking, it is necessary to evaluate first stresses (41) with $L' = L(\beta_0)$, $\underset{\sim}{\ell}' = \underset{\sim}{\ell}(\beta_0)$, i.e., with material properties at the original crack density β_0. If these stresses make the left-hand side of (37) or (39) larger than unity, then an increment $d\beta$ is required to reduce L', $\underset{\sim}{\ell}'$ to the level allowed by the selected failure criterion. When (37) or (39) are called upon, it is also necessary to adjust $\bar{\sigma}_I$ and $\bar{\sigma}_{II}$ according to the current value of β.

The increment $d\beta$ caused by (40) can be evaluated by a simple iteration scheme in which β is adjusted so that the stresses (41) satisfy (27) or (29) while $\underset{\sim}{\bar{\varepsilon}}'$ and θ' are applied.

Once the new magnitude of β has been found, it is possible to evaluate all components of the current stiffness and compliance matrices L and M.

We recall that both L and $\underset{\sim}{\ell}$ are decreasing functions of β, thus the ply softens under increasing strain, but it remains elastic during

unloading and reloading to the current stress level, Figure 7. This aspect of the procedure permits evaluation of β under incremental deformation even when the critical stresses $\bar{\sigma}_I$ and $\bar{\sigma}_{II}$ in (37) are taken as independent of β. This may be advantageous in practical applications when $\bar{\sigma}_I$ and $\bar{\sigma}_{II}$ may be known only at first ply failure, i.e., at $\beta \to 0$. If the first ply failure values are taken, the predicted magnitude of β will probably exceed the actual one. Therefore, the stiffness of the ply will be underestimated and again, the model predictions will be on the safe side in most structural applications.

3.4 Results

3.4.1 Stresses in a Deforming Ply

To illustrate typical results provided by (37), consider a graphite-epoxy ply with properties given in Table I. The ply is deformed by prescribed strains ε_{22} and ε_{23} in several radial directions, while stresses are adjusted so that $\sigma_{11} = \sigma_{12} = \sigma_{13} = \sigma_{33} = 0$. For greater clarity of presentation, the ply strengths are taken as constant:

$$\bar{\sigma}_I = \bar{\sigma}^{cr}_{22} = 28.44 \text{ MPa}, \qquad \bar{\sigma}_{II} = \bar{\sigma}^{cr}_{23} = 37.95 \text{ MPa}$$

These values were measured for first ply failure of an unconstrained ply, hence they represent relatively low strengths.

The results appear in Figure 8. In each case, the applied strain is plotted on the horizontal axis, the average stresses and crack densities on the vertical. The constant strengths levels are plotted as well. It is easy to see that if strengths were increasing with β, then the stress components would be elevated accordingly.

A remarkable feature of these results is the strong effect of shear strain ε_{23} on crack density increase. When only shear ε_{23}, or only transverse normal strain ε_{22} is applied, one finds that β increases about twice as fast in shear when is $2\varepsilon_{23}$ compared in magnitude to ε_{22}. At the same time, the shear strength exceeds the transverse tension strength by 33%. This behavior can be related to the rate of change of

the relevant stiffnessed L_{22} and L_{44} with β. We recall from Figure 2 in [5] that L_{22} decreases with β much more rapidly than L_{44}, from comparable initial levels. Thus σ_{23} is relatively large, much larger than σ_{22} for $2\varepsilon_{23} > \varepsilon_{22}$. Even at low $\varepsilon_{23}/\varepsilon_{22}$ ratios σ_{23} keeps increasing with applied strain while σ_{22} always decreases after onset of cracking.

In addition to stress changes, the ply experiences stiffness change under deformation conditions of Figure 8. These are summarized in Figure 9.

3.4.2 Progressive Cracking in Laminated Plates

The above procedure for analysis of crack accumulation in a strained ply can be combined with laminated plate theory and thus extended to cracking laminated plates. Figure 10 illustrates stress and stiffness changes in a plate subjected to combined loads.

As in the case of a lamina, cracking in laminated plates must be analyzed in an incremental way. In many applications one cannot predict the exact loading history, or a detailed analysis may be undesirably complex. Under such circumstances, it is sufficient to estimate the maximum stiffness loss caused by the greatest possible damage in individual plies. Ply properties for this case were found, for large values of β, Section 2.4.

The effect of a fixed, uniform crack density in all plies of the laminated plate, on longitudinal (E_L) and transverse (E_T) in-plane moduli of plates of different layups is illustrated in Tables II, and III and IV [9]. It is seen that the stiffness loss caused by extensive cracking can be very significant in certain composite systems.

A comparison of the theoretical results with experimental observations is presented in Figure 11. Axial stiffness of a $(0/90_3)_s$ E-glass-epoxy plate is plotted against observed crack density for a uniaxial tension test. The experimental points and shear lag analysis were presented in [10]. The theoretical (SCM) curve was calculated with the self-consistent approximation described earlier. A very good agreement of this curve with experiments is indicated. A remarkable feature of this correlation is that the only material constants used in the analysis were the original elastic moduli of the uncracked composite. With this information the stiffness changes were evaluated for given crack density from (3) for the 90° plies, and overall laminate stiffness change was found from laminated plate theory.

Additional comparisons were made with experimental results obtained by Hwang and Hahn [3] who measured crack density as a function of applied stress or strain in AS/3501-5A laminated plate coupons in tension, and, with similar experiments reported by Ryder and Crossman [11] for laminated T300/5208 plate coupons.

Analytical predictions of crack densities in these laminated plate coupons were made as follows: First, laminated plate theory was used to calculate residual thermal stresses in each ply caused by cooldown from the curing temperature. The temperature difference was $\Delta T=147°C$ for both systems. Then ply stresses caused by a uniaxial applied load were evaluated and superimposed on the thermal residual stresses in each ply Next, (37) was rewritten for each ply with stresses $\bar{\sigma}_{22}$, $\bar{\sigma}_{23}$ taken in local ply coordinates, x_3 is parallel to local fiber direction. The $\bar{\sigma}_I$, $\bar{\sigma}_{II}$ denote critical stresses at first ply failure. The parameter, which accounts for failure mode interaction in an approximate way was taken as $g=0.1$.

Now, to determine $\bar{\sigma}_I$ and $\bar{\sigma}_{II}$ for the laminate test data shown in Figures 12 and 13, one calculates the local stress $\bar{\sigma}_{22}$ at first ply failure in the 90° ply. Since $\sigma_{23} = 0$ in this ply, one obtains $\bar{\sigma}_I$ from (37). Then, additional stress is applied to the laminate, and crack density β in the 90° ply is calculated incrementally, according to the sequence (37) to (42). The stiffness of the 90° ply gradually decreases in the process. When the applied stress reaches the magnitude required for first ply failure in the +45° ply, $\bar{\sigma}_{II}$ in this ply is again found from (37).

These results are listed in Table V as predictions (A) and (B) for the two coupons.

In a similar way, the results in Figures 14 and 15 were interpreted and provided values of $\bar{\sigma}_I$ and $\bar{\sigma}_{II}$ in predictions (C), (D) and (E), Table V.

The experimentally found values of the critical stress $\bar{\sigma}_I$ and $\bar{\sigma}_{II}$ at first ply failure in (37) are actually the sole material parameters needed to fit the data. The only additional information entering the analysis are original elastic moduli of the undamaged laminate, and the empirical factor g=0.1 in (37).

The magitudes of $\bar{\sigma}_I$ and $\bar{\sigma}_{II}$ are fairly consistent. Note that predictions (A) and (B) apply to both 0° and 45° plies in Figures 12 and 13. Differences between (A) and (B) are caused by differences in experimental data. Prediction (C) is sufficient for all plies in Figure 14, except for the -45° ply as explained below. Predictions (D) and (E) in Figure (15) are different because the data points for the two coupons are so far apart.

It would be desirable to find that one set of critical stresses fits all data for a particular system, or for the two grafite-epoxy systems of Figures 12 to 15. This is not exactly possible but we note that $\bar{\sigma}_I$ in (A) (B) and (D) are similar; ideally they should coincide since they refer to a single system. Still they are closer together than those in (D) and (E) found for not only one system, but also one layup. In fact the two coupons A1 and A2 were taken from the same laminated plate.

Therefore, one can conclude that the differences in effective ply strength at first ply failure in Table V are caused by variations in material properties that affect the experimental data.

A surprising feature of the experimental results shown in Figures 12 and 14 is that no cracks were observed in the interior -45° plies. One would certainly expect to find cracks in these layers which experience the same average strain state as the +45° plies where numerous cracks were found. In fact, the -45° plies form a single ply of double thickness, and this should make it more susceptible to matrix cracking than the +45° plies of single thickness. This phenomenon requires further study.

We note in passing that not all experimental data can be approximated with the average stress condition (37). This suggests a need for a more accurate method of evaluation of local stresses in (37).

3.5 Conclusions

1. An analytical technique has been developed for modeling of progressive transverse matrix cracking in laminated composite plates. The analysis consists of three steps. First, self-consistent estimates of laminate stiffness changes are found for a given crack density from (3) and (4). Next, the rate of crack density increase under applied load is evaluated from (37) to (42) on the basis of a selected ply failure criterion. Finally, the ply analysis is made in terms of ply stress state for a ply embedded in a laminate with several cracking plies. The instantaneous ply stresses follow from a simple adaptation of laminated plate theory.

2. A good agreement of the theory with several sets of experimental data was found. The theoretical predictions require a minimum amount of experimentally derived information, such as first ply failure stresses in the cracking ply, and elastic moduli of the undamaged laminate. No empirical parameters are required outside the ply failure criterion (37).

3. The theory makes it possible to calculate the instantaneous crack density in each ply, the instantaneous stresses in each ply of the laminate, as well as the average fiber and matrix stresses in each ply, after application of each load or strain increment to the laminate. The laminate can be subjected to combined three dimensional loading, and also to varying uniform thermal changes in the course of mechanical loading.

4. The analysis can be implemented through a simple numerical routine, even on a microcomputer. In fact, the entire procedure for each loading step is rather similar to that used in elasticity analysis of laminated plates.

ACKNOWLEDGEMENT

This work was supported by the Air Force Office of Scientific Research and monitored by Major David Glasgow, Ph.D., who provided numerous useful suggestions. Dr. Norman Laws was a consultant on this project. He contributed in a significant way to the development of self-consistent estimates of mechanical properties of cracked plies and laminates. Dr. M. Hejazi and Mr. C. J. Wung participated in various stages of this work, performed the numerical calculations and helped to make comparisons of theory with experiments.

4. REFERENCES

1. S. D. Wang and F. W. Crossman. "Initiation and Growth of Transverse Cracks and Edge Delamination in Composite Laminates. Part 1. An Energy Method," J. Composite Materials, Vol. 14 (1980) : 71.

2. G. J. Dvorak and W. S. Johnson. "Fatigue of Metal Matrix Composites," International Journal of Fracture, Vol. 16, 6 (1980) : 585.

3. D. G. Hwang, "The Proof Testing and Fatigue Behavior of Gr/Ep Laminates." D.Sc. Dissertation, Washington University, St. Louis, MO, August 1982.

4. J. Bailey, P. T. Curtis and A. Parvizi. "On the Transverse Cracking and Longitudinal Splitting Behavior of Glass and Carbon Fibre Reinforced Epoxy Cross Ply Laminates and the Effect of Poisson and Thermally Generated Strain." Proc. R. Soc. Lond. A., Vol. 366 (1979) : 599.

5. N. Laws, G. J. Dvorak and M. Hejazi. "Stiffness Changes in Unidirectional Composites Caused by Crack Systems," Mechanics of Materials, Vol. 2 (1983) : 123.

6. G. J. Dvorak, N. Laws, and M.Hejazi. "Matrix Cracking in Unidirectional Composites," 1983 Advances in Aerospace Structures, Materials, and Dynamics, ASME, Vol. AD-06, November 1983.

7. G. J. Dvorak, N. Laws and M. Hejazi, "Analysis of Progressive Matrix Cracking in Composite Laminates. I. Thermoelastic Properties of a Unidirectional Composite Ply with Cracks," to appear in J. Composite Materials, 1985.

8. H. T. Hahn and T. Johannesson, "Fracture of Unidirectional Composites, Theory and Applications," in Mechanics of Composite Materials - 1983, G. J. Dvorak, editor, AMD-Vol. 58:135, ASME, New York, 1983.

9. N. Laws and G. J. Dvorak, "The Loss of Stiffness of Cracked Laminates," to appear in "Fundamentals of Deformation and Fracture," presented at the J. D. Eshelby Memorial Symposium, University of Sheffield, April 1984.

10. A. L. Highsmith and K. L. Reifsnider, "Stiffness-Reduction Mechanisms in Composite Laminates," ASTM-STP 775, p. 103-117, 1982.

11. J. T. Ryder and R. W. Crossman, "A Study of Stiffness, Residual Strength and Fatigue Life Relationships for Composite Laminates," NASA Contract Report CR-172211, 1983.

Table I. Constituent Properties and Compliances of the T300 Gr-Ep System

	Unit	E_{33}	G_{31}	ν_{31}	E_{11}	G_{12}	Symmetry
Fiber (T300)	10^3ksi	33.00	3.36	0.410	2.25	0.78	Transversely Isotropic
	10^3MPa	227.5	23.2		15.5	5.4	
Matrix (Epoxy)	10^3ksi	0.50	0.19	0.350	0.50	0.19	Isotropic
	10^3MPa	3.4	1.3		3.4	1.3	

Composite Compliances:

Compliance	c_f=0.2	c_f=0.4	c_f=0.6
M^o_{11}	0.2069	0.1595	0.1192
M^o_{12}	-0.1037	-0.0779	-0.0561
M^o_{13}	-0.0075	-0.0041	-0.0028
M^o_{22}	0.2069	0.1595	0.1192
M^o_{23}	-0.0075	-0.0041	-0.0028
M^o_{33}	0.0207	0.0107	0.0073
M^o_{44}	0.5108	0.2726	0.1244
M^o_{55}	0.5108	0.2726	0.1244
M^o_{66}	0.6211	0.4746	0.3506

All values are in units of $(10^3 \text{ MPa})^{-1}$

40% T300/5208

% OF UNCRACKED MODULUS E_L

Lay-up \ β	0.2	0.6	1.0
$(0_4, 90)$	100	99	99
$(0_2, 90)$	99	98	97
$(0, 90)$	98	96	95
$(0, 90_2)$	97	92	90
$(0, 90_4)$	95	86	82
$(0_2, \pm 45)$	99	97	95
$(0, \pm 45)$	98	94	92
$(0, (\pm 45)_2)$	97	91	86
(± 45)	91	74	59
$(0_2, \pm 75)$	99	96	95
$(0_2, \pm 60)$	99	97	95
$(0_2, \pm 30)$	99	97	95
$(0_2, \pm 15)$	100	99	99

40% T300/5208

% OF UNCRACKED MODULUS E_T

Lay-up \ β	0.2	0.6	1.0
$(0_2, \pm 45)$	97	91	87
$(0, \pm 45)$	96	89	84
$(0, (\pm 45)_2)$	95	87	80
(± 45)	91	74	59
$(0_2, \pm 75)$	100	99	99
$(0_2, \pm 60)$	99	97	96
$(0_2, \pm 30)$	92	79	71
$(0_2, \pm 15)$	88	69	59

Table II. Theoretical predictions of relative changes in axial (E_L) and transverse (E_T) Young's moduli of laminated plates at given values of crack density β in all plies.

60% E-GLASS/EPOXY

% OF UNCRACKED MODULUS E_L

Lay-up \ β	0.2	0.6	1.0
$(0_2, \pm 45)$	92	83	75
$(0, \pm 45)$	88	75	63
$(0, (\pm 45)_2)$	84	67	50
(± 45)	77	51	25

60% E-GLASS EPOXY

% OF UNCRACKED MODULUS E_T

Lay-up \ β	0.2	0.6	1.0
$(0_2, \pm 45)$	86	73	64
$(0, \pm 45)$	82	66	53
$(0, (\pm 45)_2)$	80	60	44
(± 45)	77	51	25

Table III. Theoretical predictions of relative changes in axial (E_L) and transverse (E_T) Young's moduli of laminated plates at given values of crack density β in all plies.

40% BORON/ALUMINIUM

% OF UNCRACKED MODULUS E_L

Lay-up \ β	0.2	0.4	0.6
$(0_4, 90)$	96	93	91
$(0_2, 90)$	93	87	83
$(0, 90)$	89	80	73
$(0, 90_2)$	85	71	62
$(0, 90_4)$	80	64	51
$(0_4, \pm 45)$	96	93	90
$(0_2, \pm 45)$	94	89	85
$(0, \pm 45)$	91	84	78
$(0, (\pm 45)_2)$	89	80	73

40% BORON/ALUMINIUM

% OF UNCRACKED MODULUS E_T

Lay-up \ β	0.2	0.4	0.6
$(0_4, \pm 45)$	95	90	87
$(0_2, \pm 45)$	93	86	81
$(0, \pm 45)$	90	82	75
$(0, (\pm 45)_2)$	88	78	70

Table IV. Theoretical predictions of relative changes in axial (E_L) and transverse (E_T) Young's moduli of laminated plates at given values of crack density β in all plies.

PREDICTION	$\bar{\sigma}_I$ MPa	$\bar{\sigma}_{III}$ MPa	MATERIAL	LAYUP	COUPON
A	64.5	73.5	AS/3501-5A	$(0_2/90/\pm45)_s$	A-b-4
B	64.5	125			A-b-6
C	83	105	T300/5208	$(0/90/\pm45)_s$	
D	45	100		$(0_2/90_4)_s$	A2
E	70	100			A1

Table V. Effective Ply Strength At First Ply Failure

TWO-PHASE MODEL OF A CRACKED LAMINA

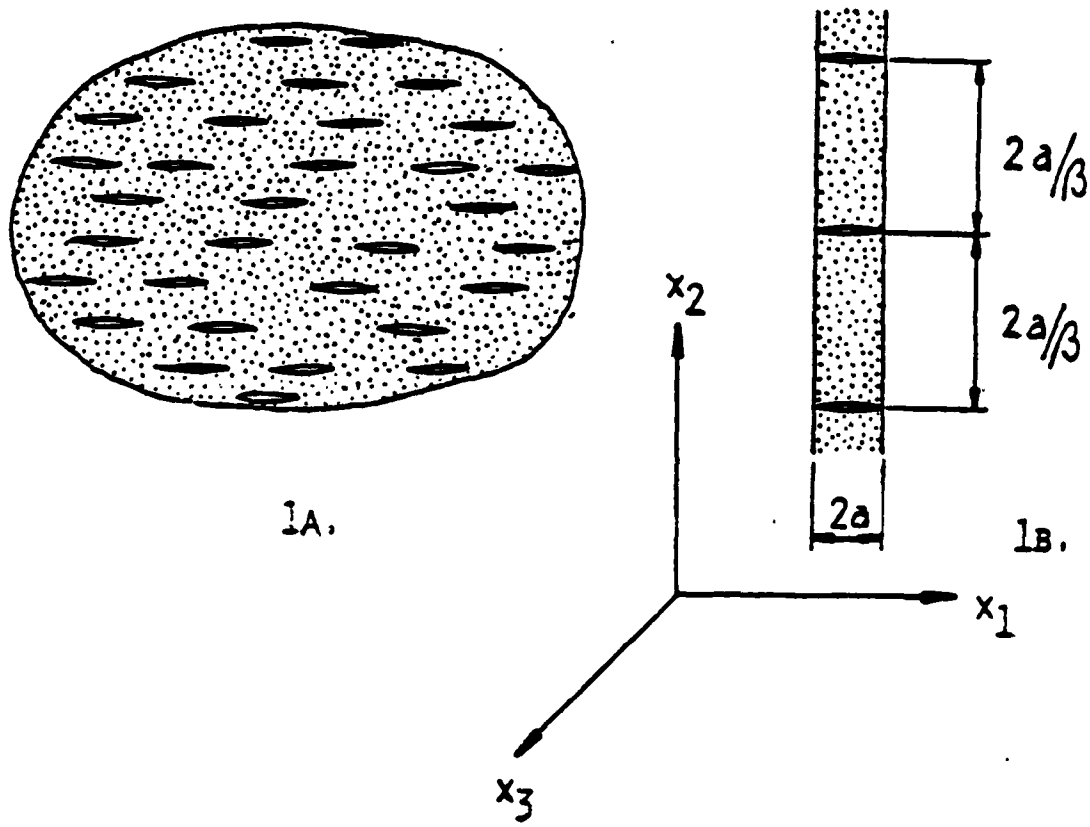

Figure 1.

1A. An infinite fibrous medium with aligned slit cracks,

1B. A fiber lamina with parallel slit cracks.

THREE-PHASE MODEL OF A CRACKED LAMINA

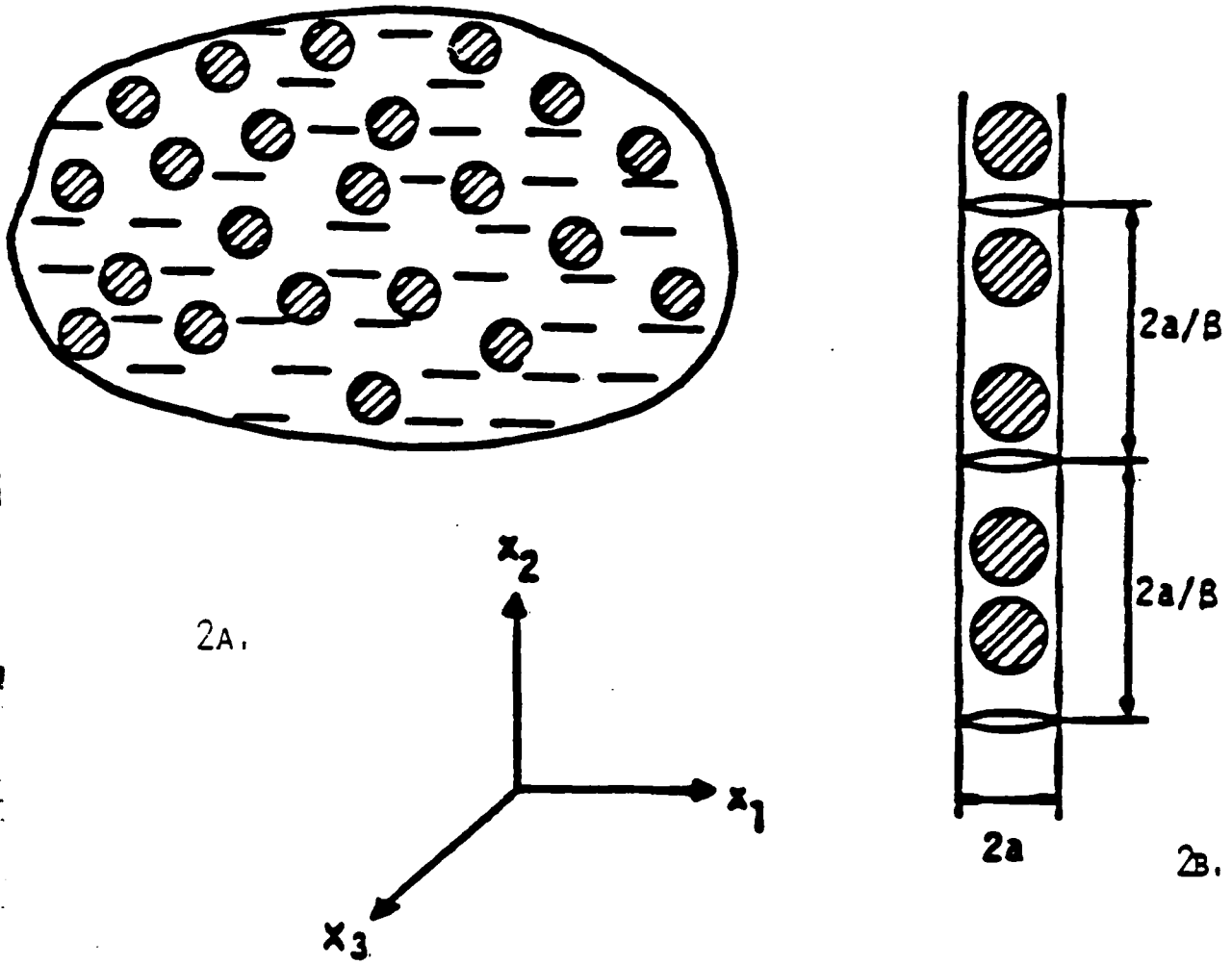

Figure 2.

2A. An infinite medium with aligned fibers and slit cracks,

2B, A fiber monolayer with cracks.

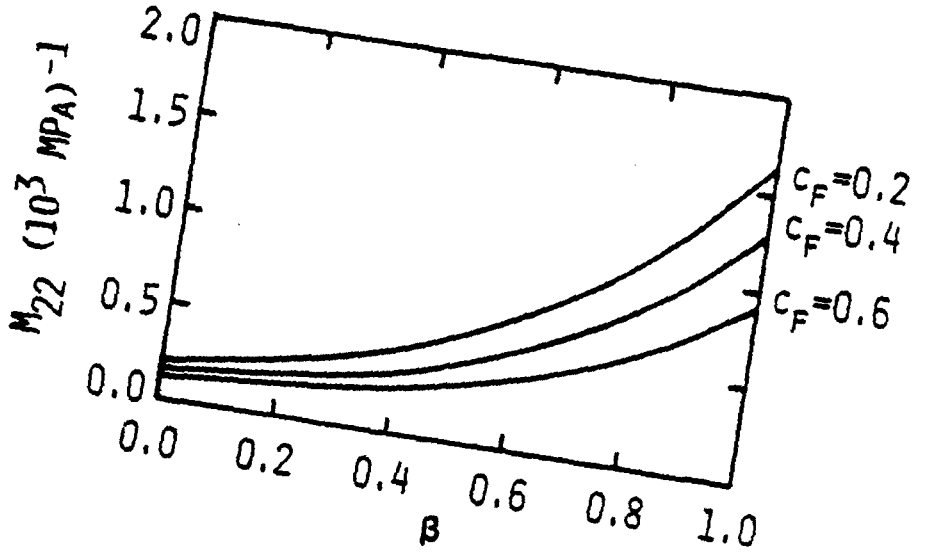

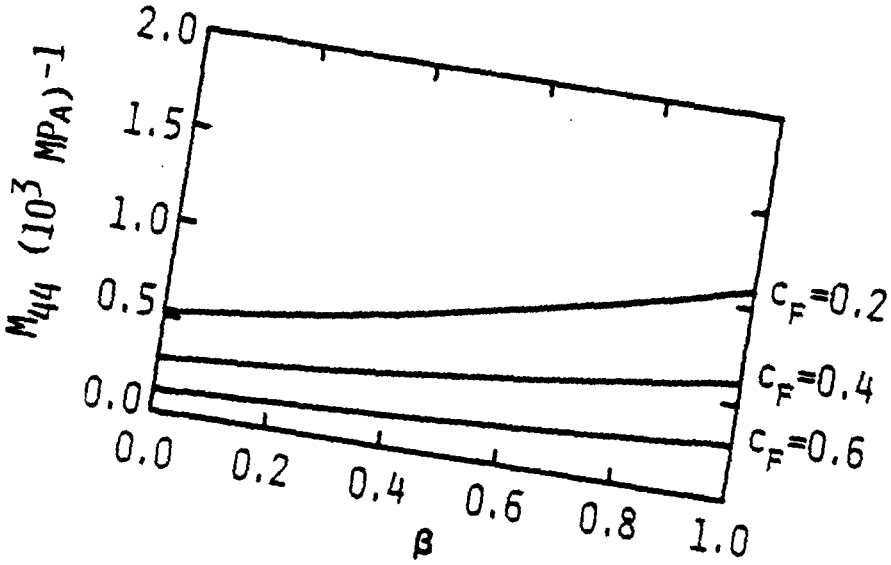

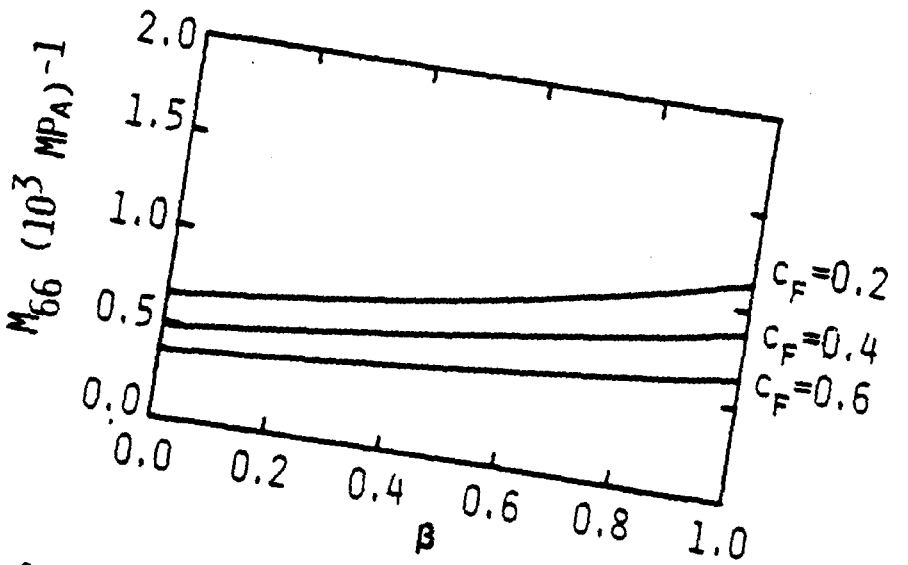

Figure 3. Compliance changes in the T300 Gr-Ep system caused by cracks of density β.

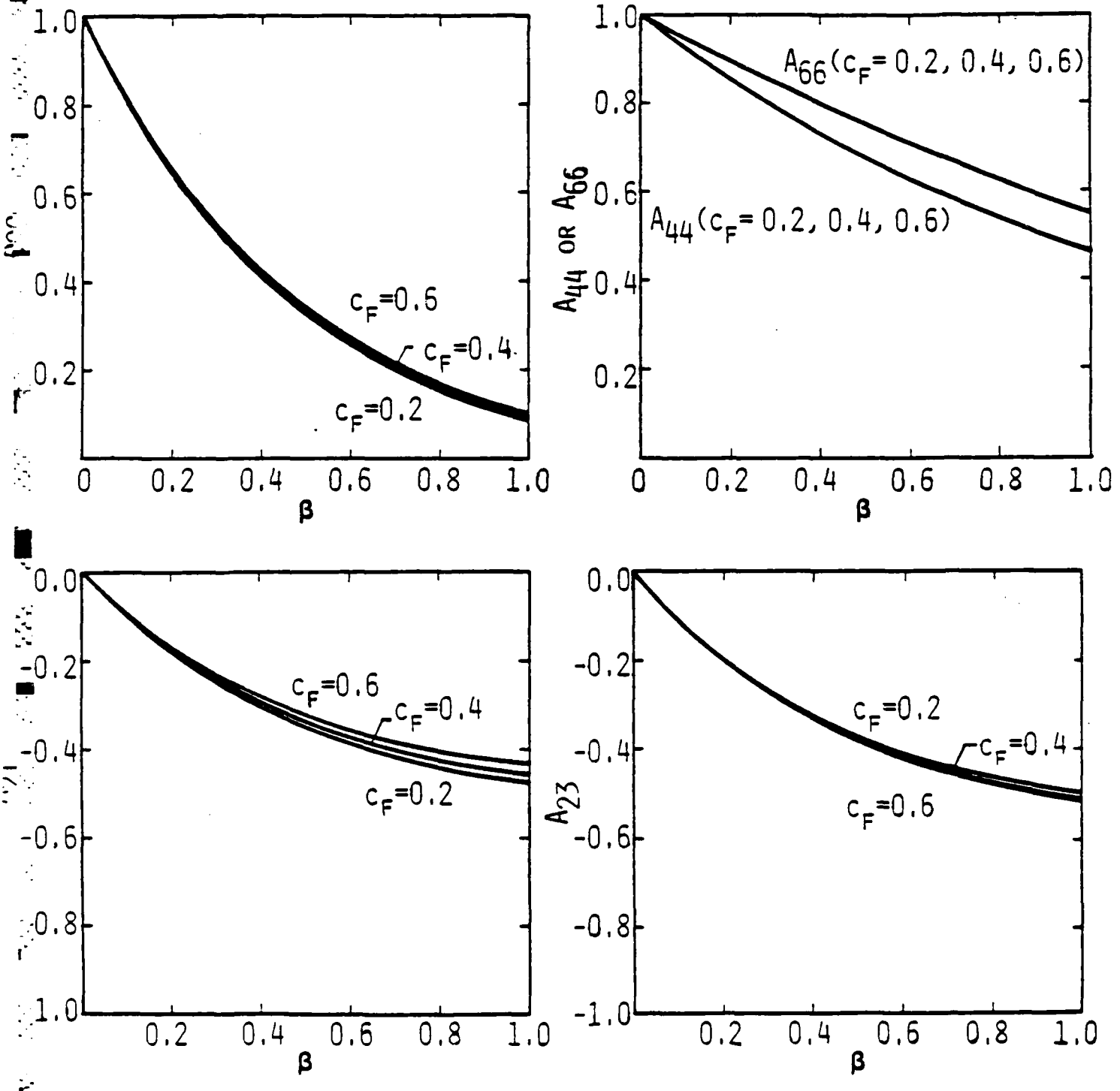

Figure 4. Changes in strain concentration factor components in composite "matrix" caused by cracks of density β (T300 Gr-Ep).

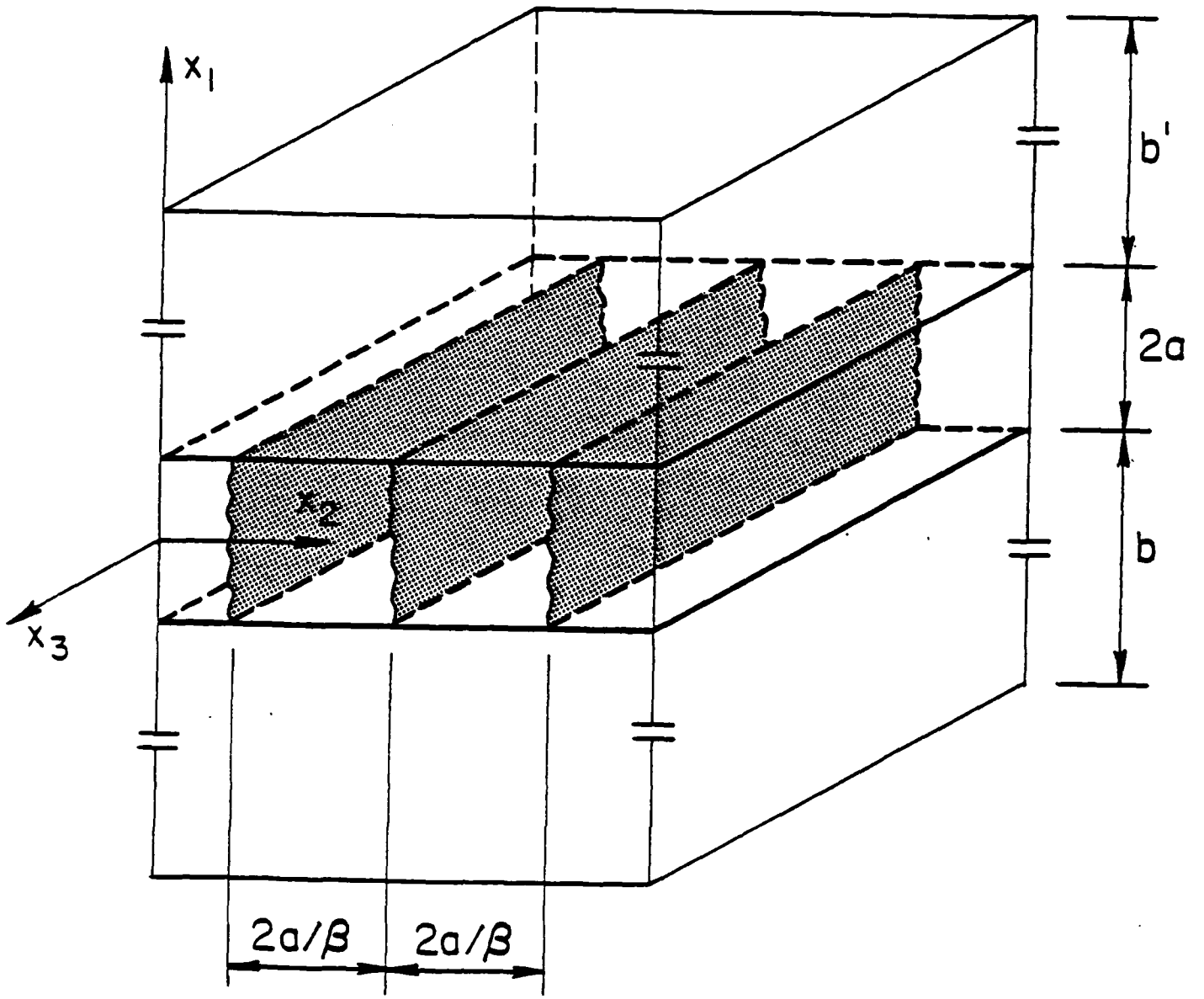

Figure 5. Slit crack system in a uniformly strained composite ply. Fibers and cracks are aligned with x_3 axis.

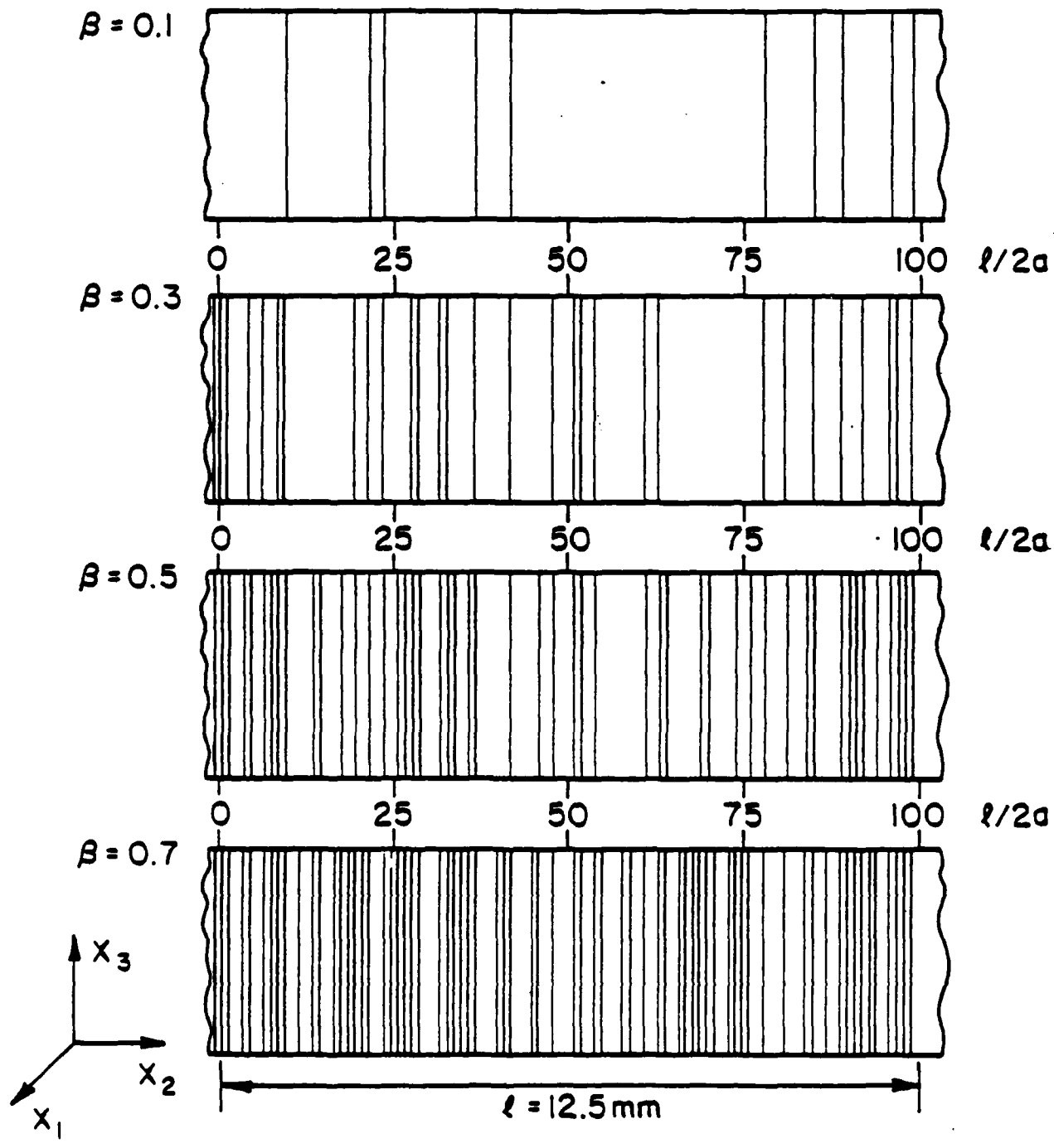

Figure 6. Random distribution of matrix cracks in a progressively cracking, 0.125 mm thick ply.

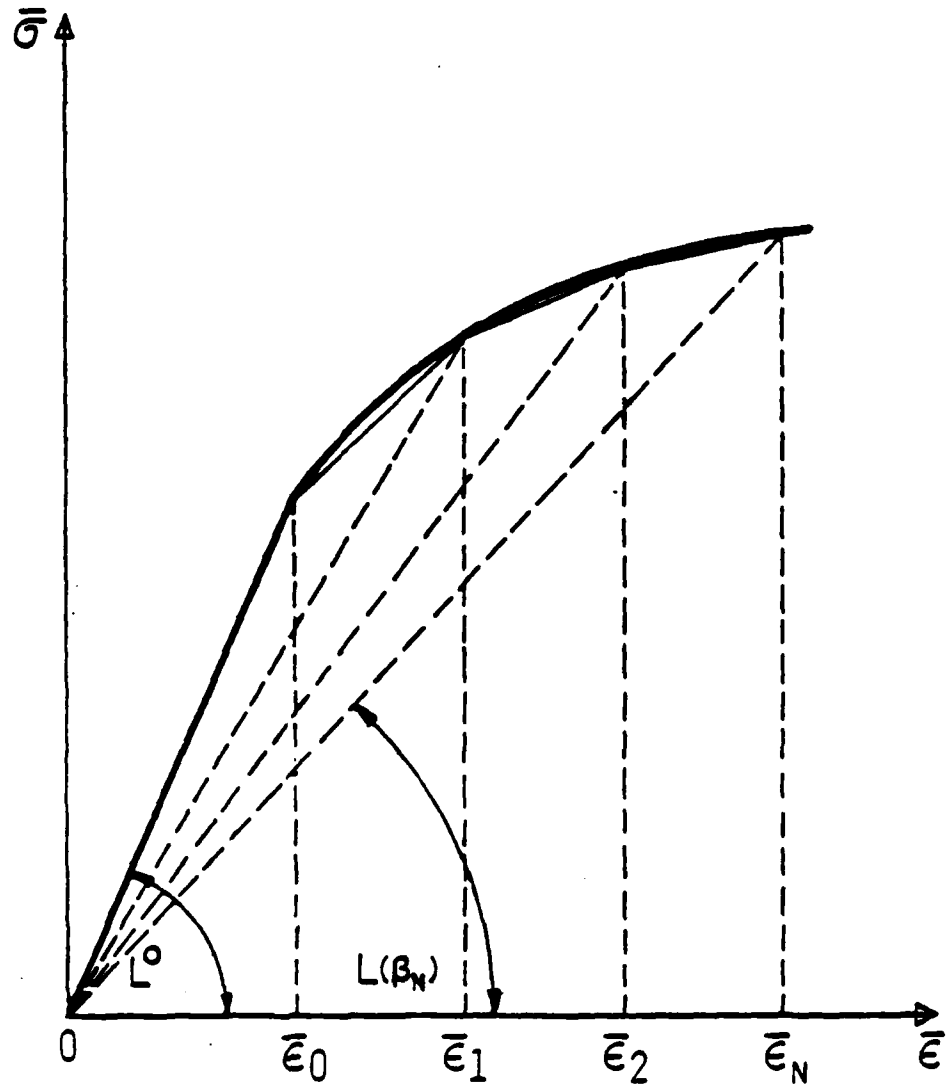

Figure 7. Schematic illustration of stiffness change of a cracking lamina.

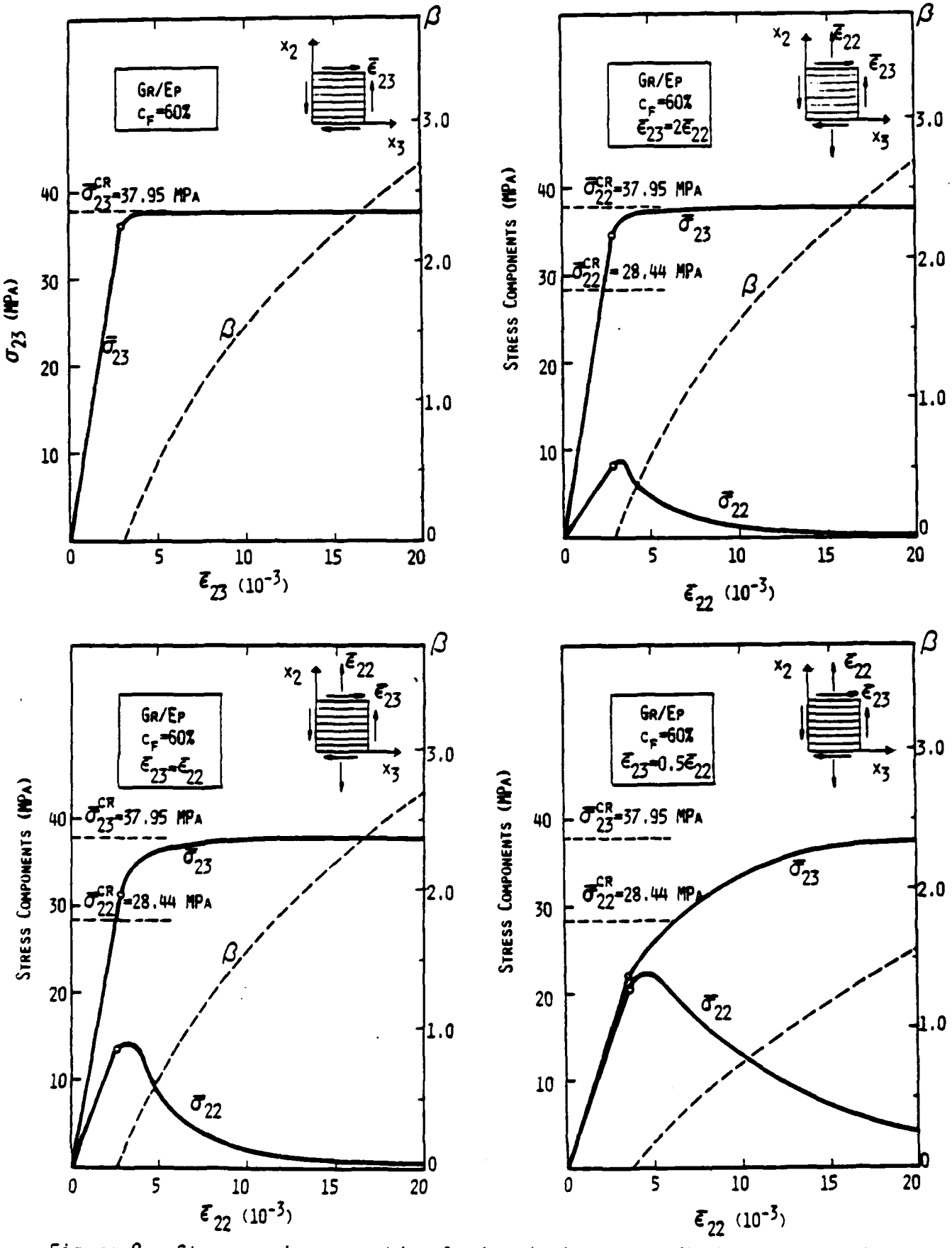

Figure 8. Stresses in a cracking lamina during prescribed proportional straining. Plane stress, $\sigma_{11} = \sigma_{33} = 0$.

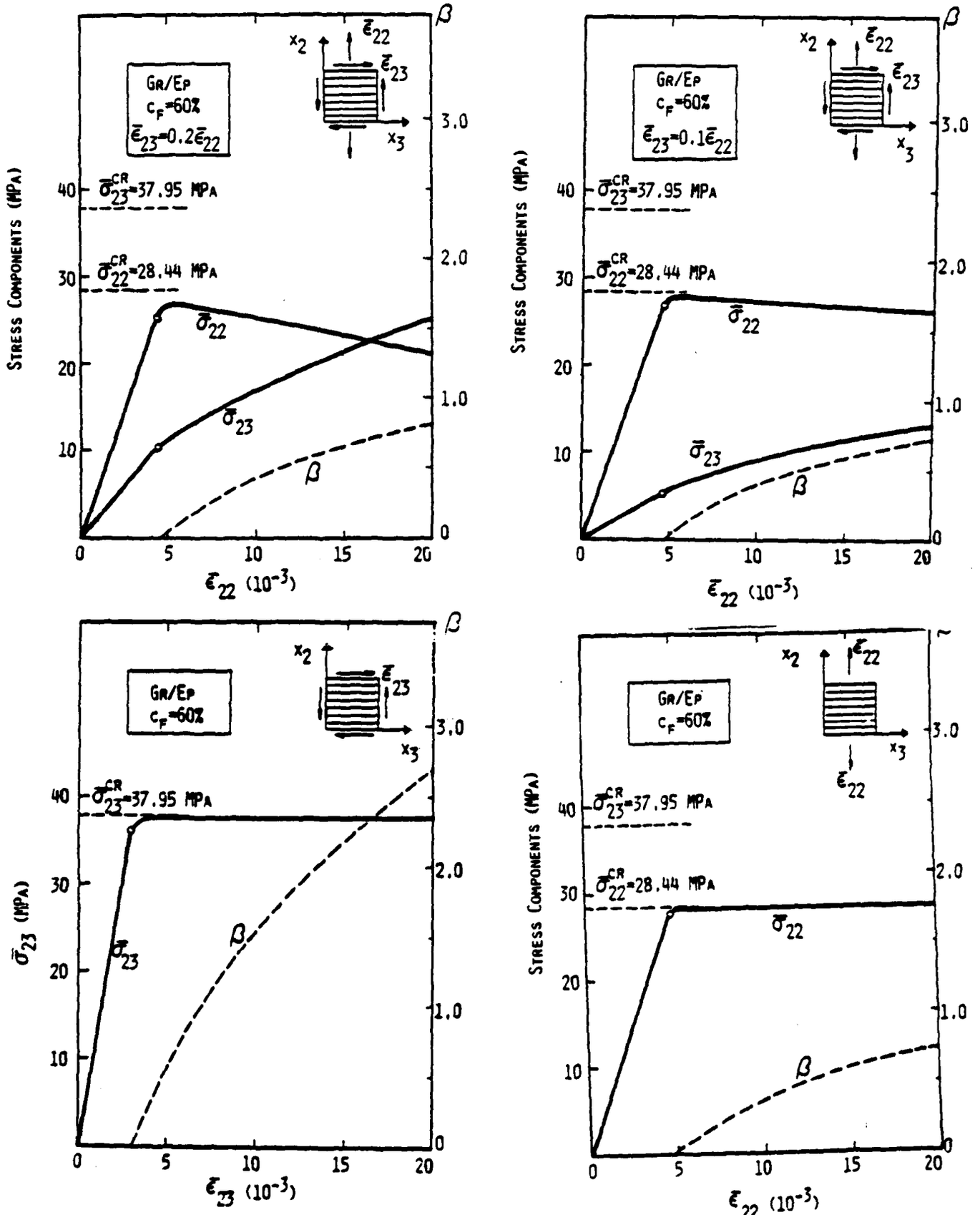

Figure 8 (Continued)

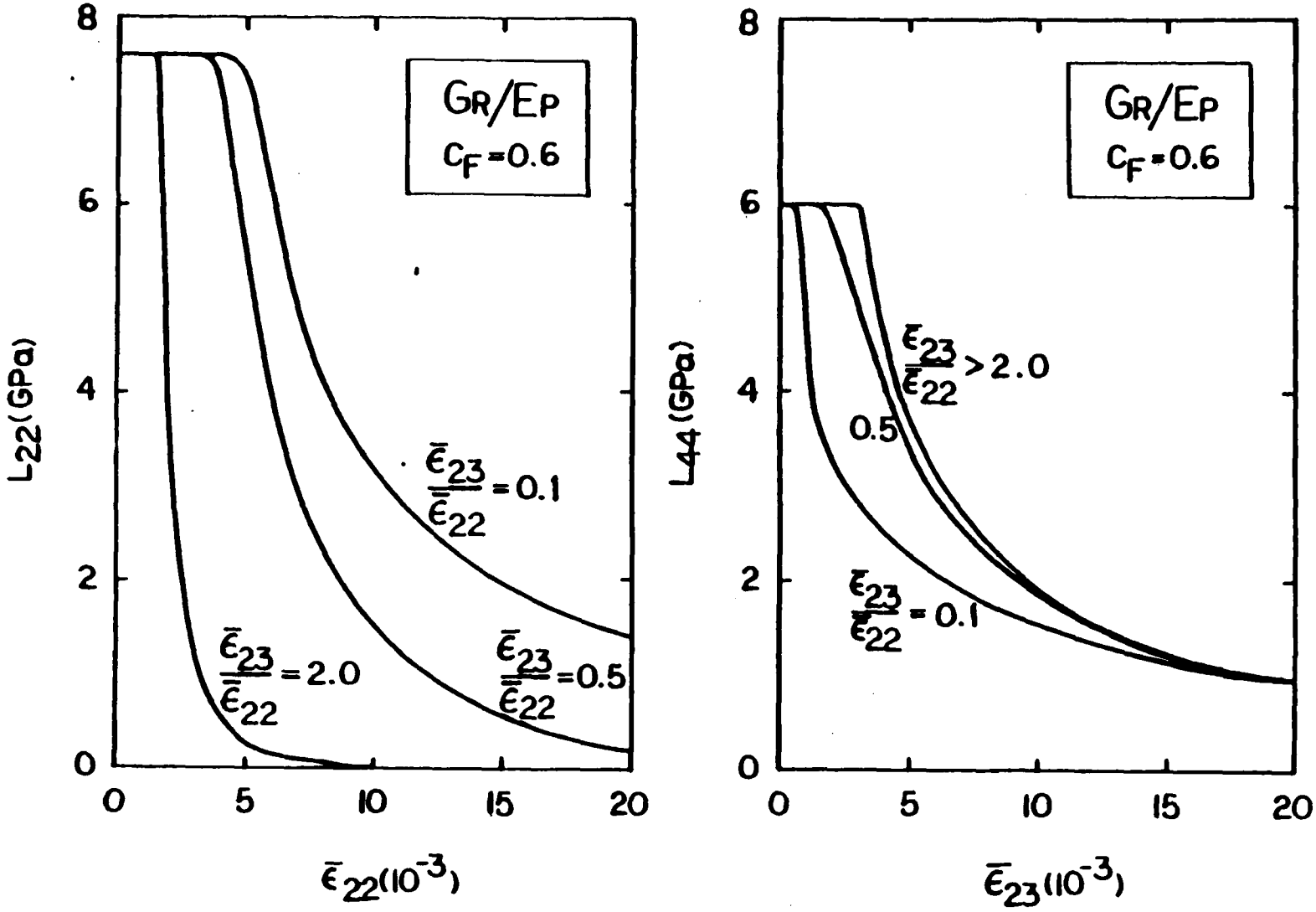

Figure 9. Stiffness changes in the graphite-epoxy ply of Figure 3, as functions of applied strain.

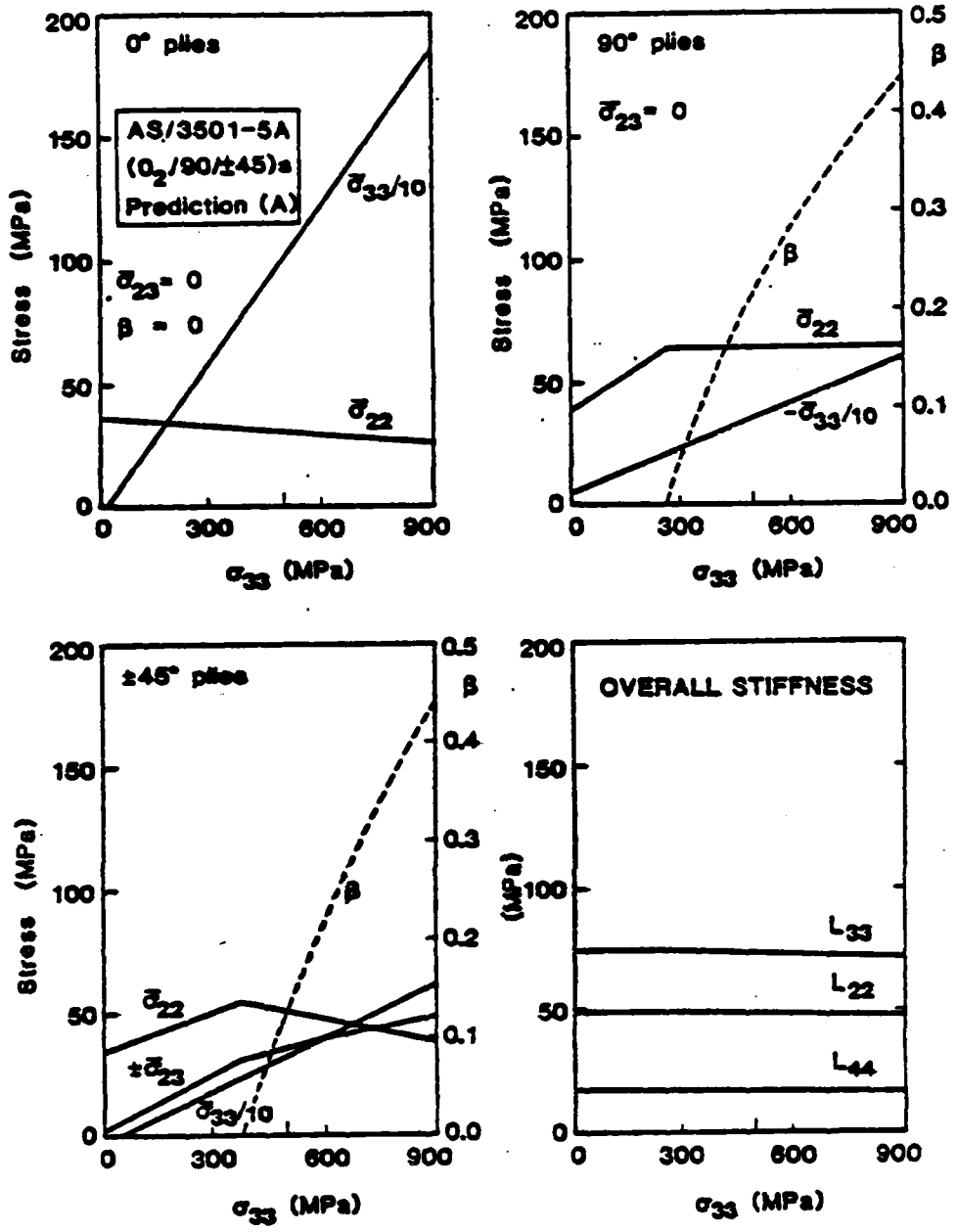

Figure 10. Calculated changes in ply stresses $\bar{\sigma}_{ij}$ and plate stiffnesses L_{ij} in a graphite-epoxy plate loaded in simple tension σ_{33} in the 0° direction. All stresses are in local ply coordinates, the fiber direction coincides with local $\bar{x}_3$ axis of a ply.

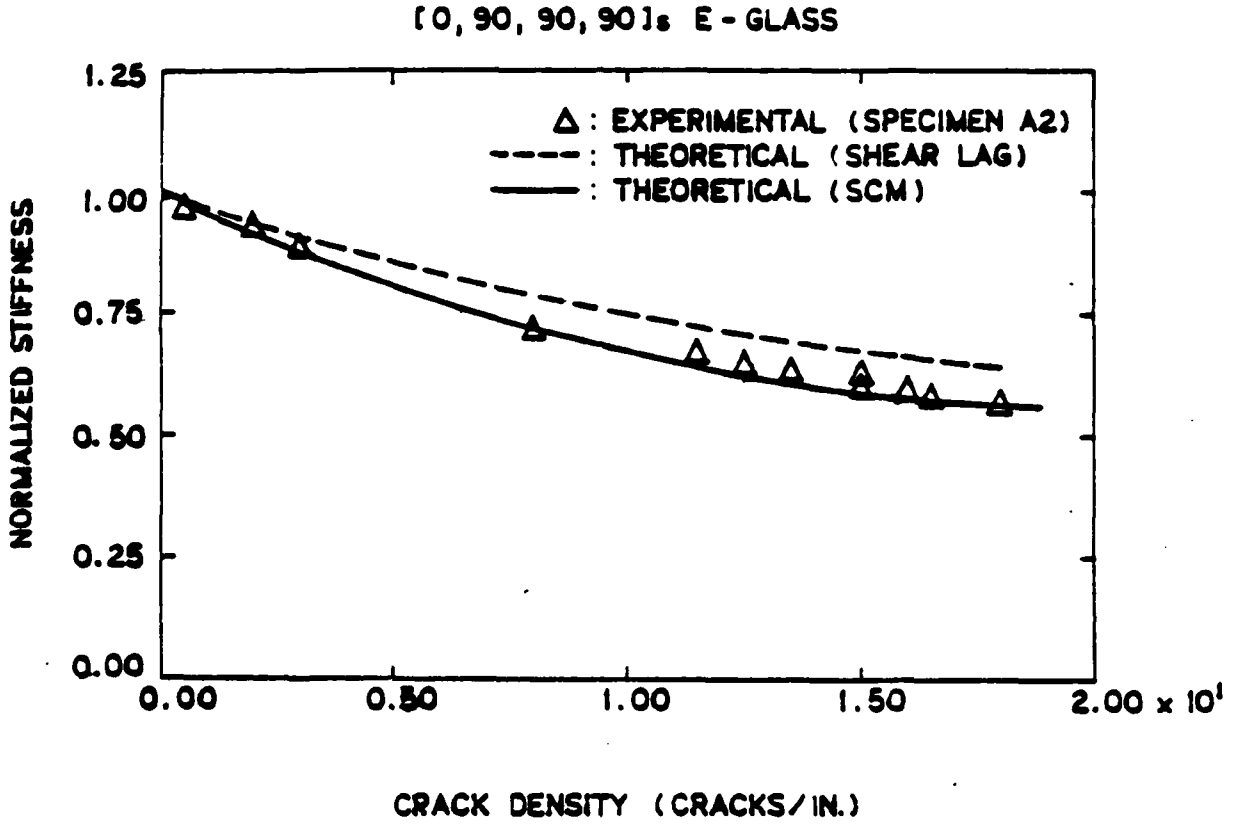

Figure 11. Comparison of experimentally observed stiffness changes and crack densities [11] with theoretical predictions. The (SCM) curve was calculated from the self-consistent estimate of stiffness in 90° plies, Equation (3).

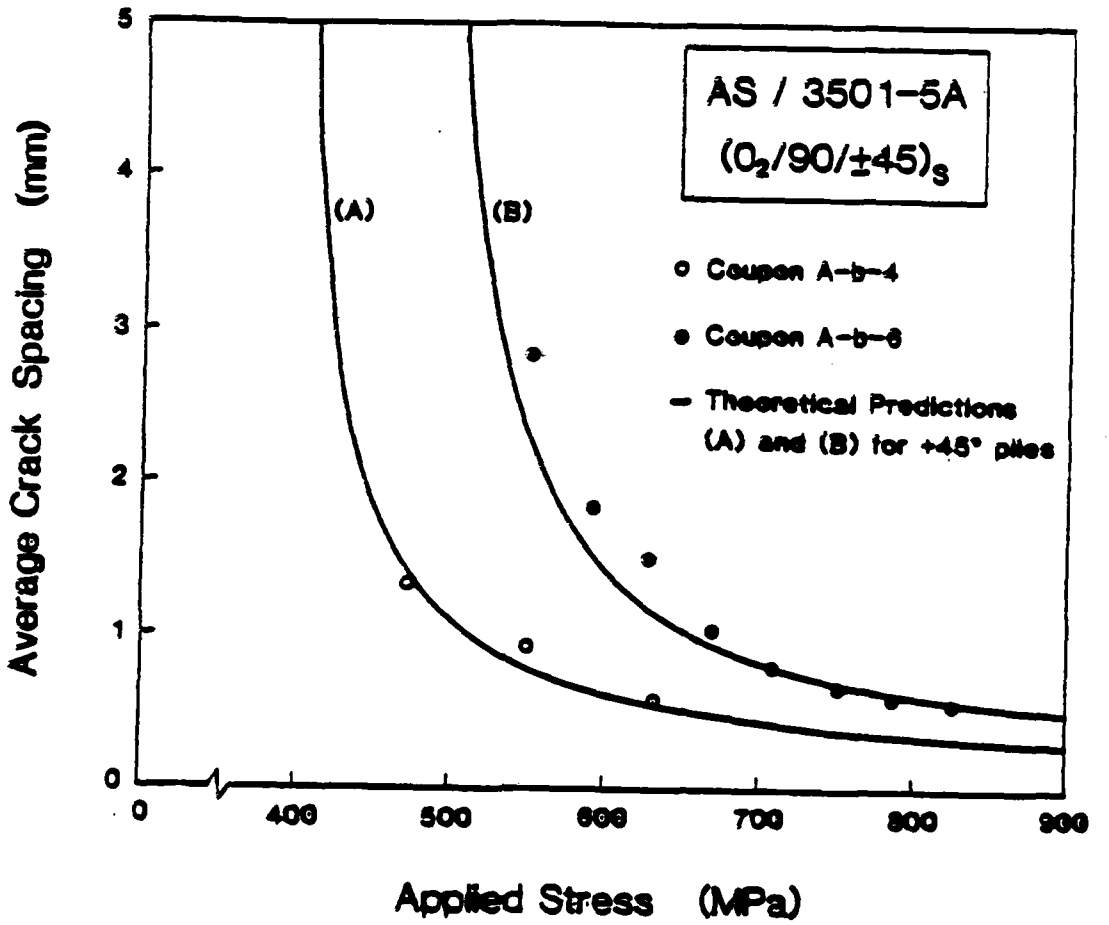

Figure 12. Comparison of Predicted and Observed Average Crack Spacing in a Laminated Plate Subjected to Uniaxial Tension. Experimental Data from Hwang and Hahn (1982).

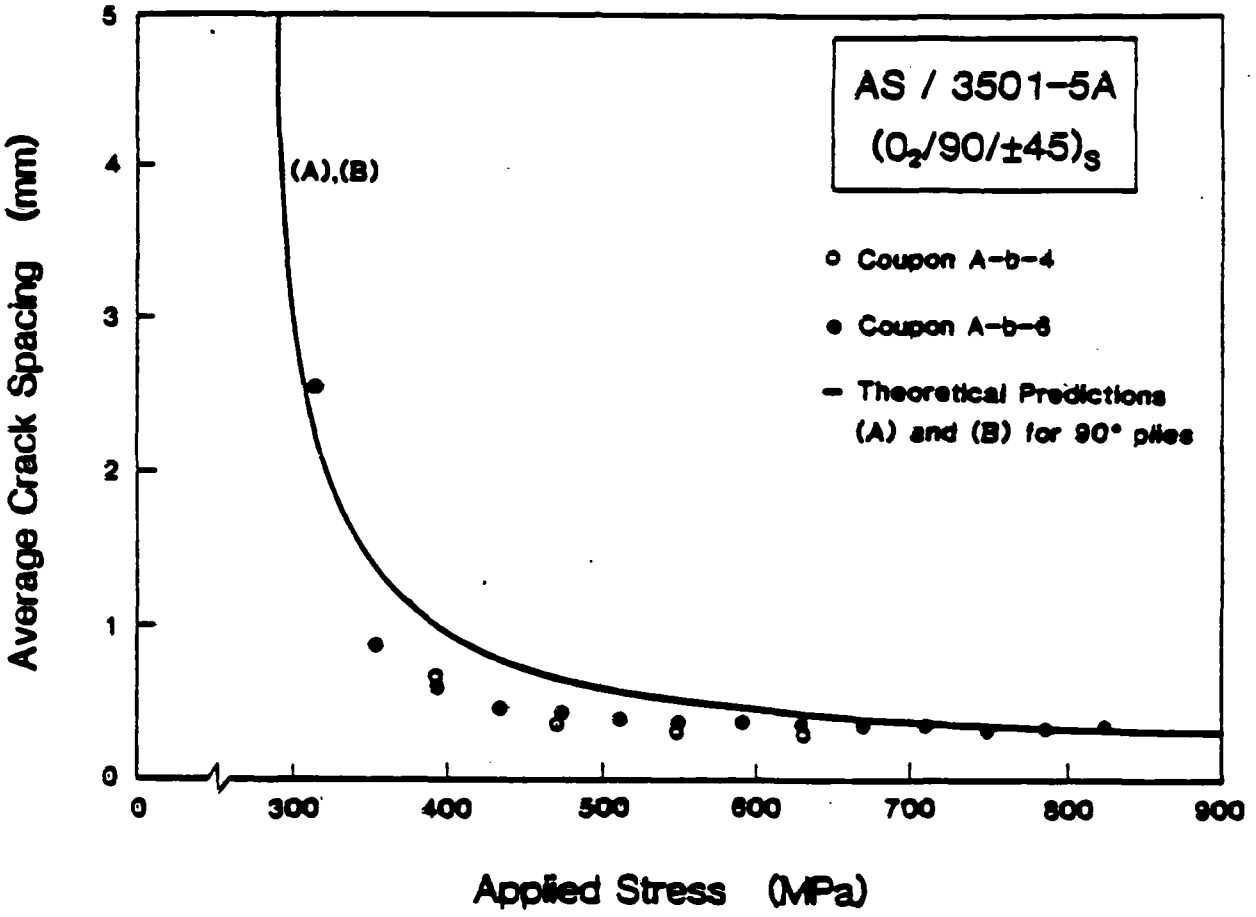

Figure 13. Comparison of Predicted and Observed Average Crack Spacing in a Laminated Plate Subjected to Uniaxial Tension. Experimental Data from Hwang and Hahn (1982).

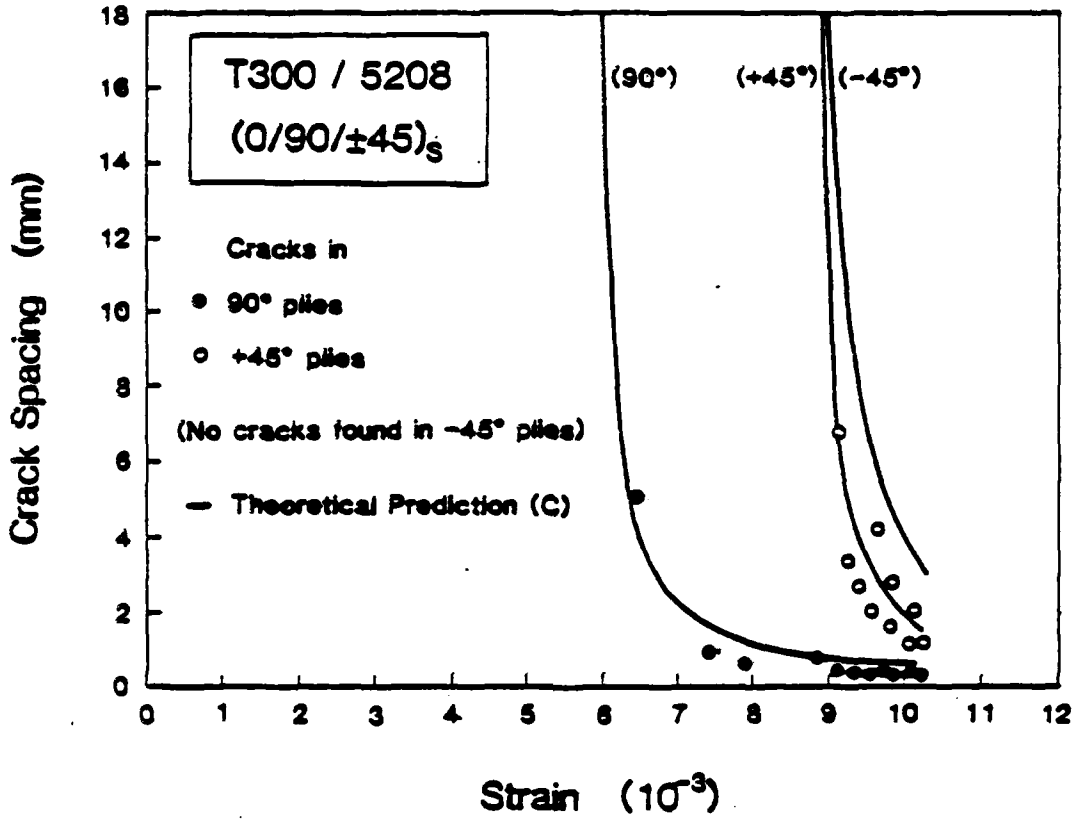

Figure 14. Comparison of Predicted and Observed Average Crack Spacing in a Laminated Plate Subjected to Uniaxial Extension. Experimental Data from Ryder and Crossman (1984).

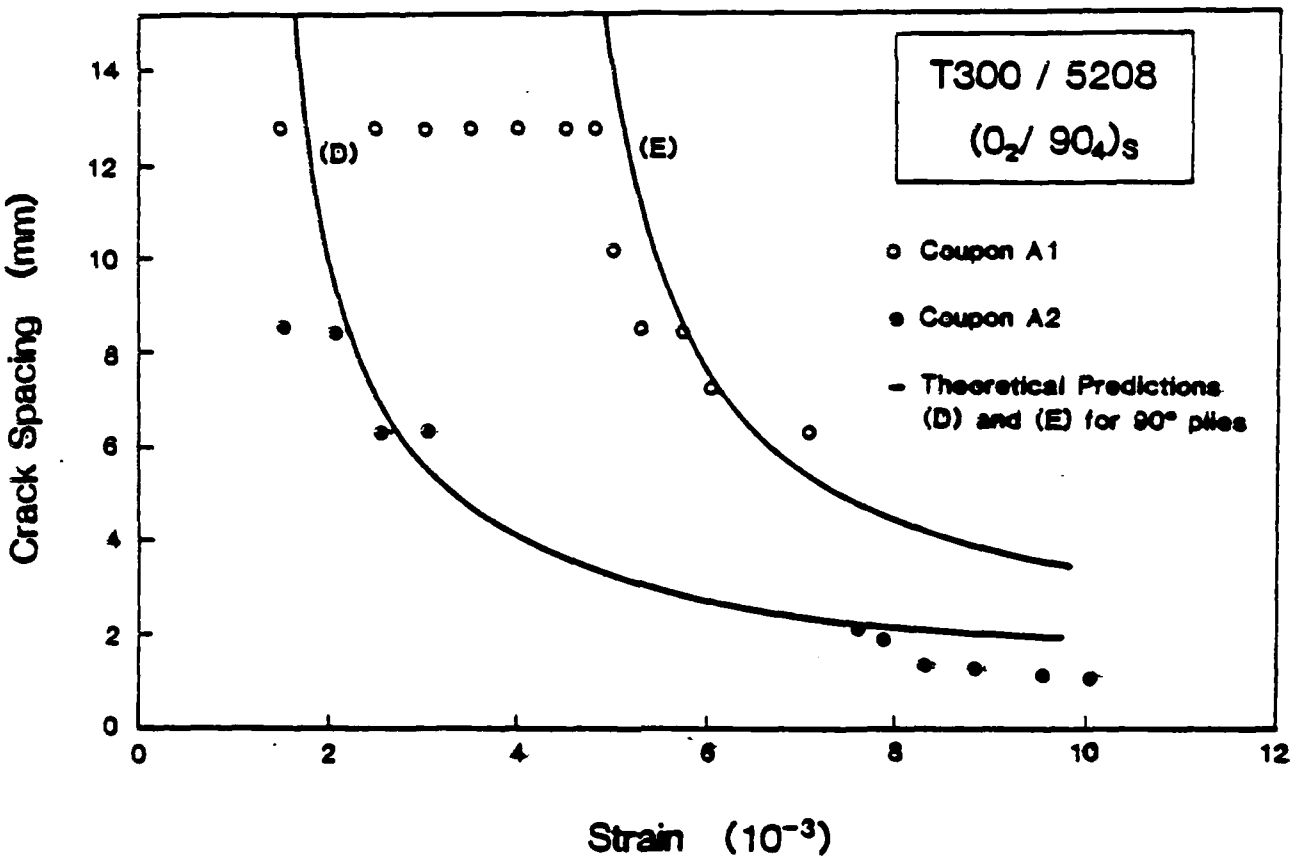

Figure 15. Comparison of Predicted and Observed Average Crack Spacing in a Laminated Plate Subjected to Uniaxial Extension. Experimental data from Ryder and Crossman (1984).

5. LIST OF PUBLICATIONS

N. Laws, G. J. Dvorak and M. Hejazi, "Stiffness Changes in Unidirectional Composites Caused by Crack Systems," Mechanics of Materials, Vol. 2 (1983) : 123.

G. J. Dvorak N. Laws and M. Hejazi, "Matrix Cracking in Unidirectional Composites," 1983 Advances in Aerospace Structures, Materials, and Dynamics, ASME, Vol. AD-06, November 1983.

G. J. Dvorak, N. Laws and M. Hejazi, "Analysis of Progressive Matrix Cracking in Composite Laminates. I. Thermoelastic Properties of a Unidirectional Composite Ply with Cracks," to be published J. Composite Materials, 1985.

N. Laws and G. J. Dvorak, "The Loss of Stiffness of Cracked Laminates," to appear in "Fundamentals of Deformation and Fracture," presented at the J. D. Eshelby Memorial Symposium, University of Sheffield, April 1984.

G. J. Dvorak and N. Laws, "Analysis Matrix Cracking in Composite Laminates: Theory and Experiment," 1984 Advances in Aerospace Sciences and Engineering, Structures, Materials, Dynamics, and Space Station Propulsion - AD-08, ASME, 1984, pp. 59-78.

6. LIST OF PROFESSIONAL PERSONNEL

Dr. G. J. Dvorak, Principal Investigator

Dr. N. Laws, Consultant

Dr. M. Hejazi, Consultant

Mr. Bruce Jenson, Graduate Student

Mr. C. J. Wung, Graduate Student

Mr. C. Z. Hu, Graduate Student

Degrees Granted - Burce Jenson, M.E., 1984.

7. PRESENTATIONS

Colloque International du CNRS n° 351, Failure Criteria of Structured Media, Villiard de Lans, France, June 1983.

Mechanics of Composites Review, Wright-Patterson AFB, Dayton, OH, October 1983.

1983 Symposium on Advances in Aerospace, Structures, Materials and Dynamics, ASME, Boston, MA, November 1983.

Eshelby Memorial Symposium, "Fundamentals of Deformation and Fracture," University of Sheffield, 2-5 April 1984.

16th IUTAM: International Congress on Theoretical and Applied Mechanics, Lyngby, Denmark, August 24, 1984.

ASME Winter Annual Meeting, New Orleans, December 10, 1984.

UNCLASSIFIED
SECURITY CLASSIFICATION OF THIS PAGE (When Data Entered)

REPORT DOCUMENTATION PAGE	READ INSTRUCTIONS BEFORE COMPLETING FORM
1. REPORT NUMBER AFOSR-TR- 85-1064	2. GOVT ACCESSION NO. AD-A162 220
3. RECIPIENT'S CATALOG NUMBER	
4. TITLE (and Subtitle) ANALYSIS OF PROGRESSIVE MATRIX CRACKING IN COMPOSITE LAMINATES	5. TYPE OF REPORT & PERIOD COVERED FINAL REPORT 9/1/82-8/31/84
	6. PERFORMING ORG. REPORT NUMBER
7. AUTHOR(s) George J. Dvorak	8. CONTRACT OR GRANT NUMBER(s) AFOSR-82-0308
9. PERFORMING ORGANIZATION NAME AND ADDRESS Department of Civil Engineering University of Utah	10. PROGRAM ELEMENT, PROJECT, TASK AREA & WORK UNIT NUMBERS 61102F/2302/B2
11. CONTROLLING OFFICE NAME AND ADDRESS AFOSR/NA David A. Glasgow Building 410 Bolling AFB, D.C. 20332	12. REPORT DATE March 31, 1985
	13. NUMBER OF PAGES 66
14. Same as # 11	15. SECURITY CLASS. (of this report) Unclassified
	15a. DECLASSIFICATION/DOWNGRADING SCHEDULE

16. Approved for public release; distribution unlimited.

17. DISTRIBUTION STATEMENT (of the abstract entered in Block 20, if different from Report)

Approved for public release/distribution unlimited.

18. SUPPLEMENTARY NOTES

19. KEY WORDS (Continue on reverse side if necessary and identify by block number)

Composite materials, cracking, damage accumulation

20. ABSTRACT (Continue on reverse side if necessary and identify by block number)

A summary of recent results is presented on the subject of progressive ply cracking in fibrous laminates. First, evaluation of stiffness changes caused by systems of aligned slit cracks which are parallel to the fiber direction in a unidirectional composite lamina is discussed. Results obtained by the self-consistent method are presented. Next, a procedure for estimating instantaneous crack densities and stiffness changes in a lamina subjected to prescribed strain history is outlined. These results are extended to analysis of laminated composite plates under in-plane stresses. Specific examples and comparisons of analytical and experimental results are presented for two graphite-epoxy systems.

DD FORM 1 JAN 73 1473 EDITION OF 1 NOV 65 IS OBSOLETE

UNCLASSIFIED
SECURITY CLASSIFICATION OF THIS PAGE (When Data Entered)

END

FILMED

1-86

DTIC